UC Berkeley

Title
Polarization contributions to intermolecular interactions revisited with fragment electric-field response functions

Permalink
https://escholarship.org/uc/item/7dm5r7jh

Journal
The Journal of Chemical Physics, 143(11)

ISSN
0021-9606

Authors
Horn, Paul R
Head-Gordon, Martin

Publication Date
2015-09-21

DOI
10.1063/1.4930534

Polarization contributions to intermolecular interactions revisited with fragment electric-field response functions

Paul R. Horn[1, a)] and Martin Head-Gordon[1, b)]

Kenneth S. Pitzer Center for Theoretical Chemistry, Department of Chemistry, University of California, Berkeley, CA 94720 and Chemical Sciences Division Lawrence Berkeley National Laboratory Berkeley, CA, 94720 Phone: 510-642-5957 Fax: 510-643-1255

The polarization energy in intermolecular interactions treated by self-consistent field (SCF) electronic structure theory is often evaluated using a constraint that the atomic orbital (AO) to molecular orbital transformation is blocked by fragments. This approach is tied to AO basis sets, overestimates polarization energies in the overlapping regime, particularly in large AO basis sets, and lacks a useful complete basis set limit. These problems are addressed by the construction of polarization subspaces based on the responses of isolated fragments to weak electric fields. These subspaces are spanned by fragment electric-field response functions (FERFs), which can capture effects up to the dipole (D), or quadrupole (DQ) level, or beyond. Schemes are presented for the creation of both non-orthogonal and orthogonal fragment subspaces, and the basis set convergence of the polarization energies computed using these spaces is assessed. Numerical calculations for the water dimer, water-Na^+, water-Mg^{2+}, water-F^- and water-Cl^- show that the non-orthogonal DQ model is very satisfactory, with small differences relative to the orthogonalized model. Additionally, we prove a fundamental difference between the polarization degrees of freedom in the fragment-blocked approaches and in constrained density schemes. Only the former are capable of properly prohibiting charge delocalization during polarization.

I. INTRODUCTION

Energy decomposition analysis (EDA) methods in electronic structure theory[1] seek to partition interaction energies into physically meaningful contributions such as permanent electrostatics, induced electron polarization, dispersion interactions, charge transfer, Pauli repulsions, etc. Such contributions are useful for understanding the ways in which different components of a system interact and for determining modifications of a system that might lead to a desired outcome. While these physical concepts may be intuitive, their definitions are not unique, except in the regime where different fragments do not overlap. However, the interesting regime of intermolecular interactions is of course the overlapping regime! The goal of this work is to present a new definition of the energy lowering associated with polarization which has several desirable qualities that not all other definitions satisfy.

In the opinion of the authors, the following are attractive properties of an energy decomposition scheme and its corresponding definitions of terms:

1. Total interaction energy corresponds to a well-defined computational method. An EDA should subdivide the total intermolecular interaction energy calculated by a useful standard electronic structure method, such as a density functional theory, into physically interpretable contributions.

2. Basis function independence. The approach should not rely on the use of a particular type of basis function, such as atomic orbitals (AO's), but rather should be applicable to any convenient one-particle basis including plane waves, finite elements, etc, in addition to AO's.

3. Non-trivial basis set limit. In the overlapping regime it should be possible to converge each energy term to a stable and physically meaningful complete basis set limit.

4. Correct asymptotic behavior. The energy contributions must reproduce their known asymptotic behavior. For example, intermolecular polarization between neutral molecules with permanent dipoles yields an asymptotic R^{-6} dependence with known coefficient.

5. Quantum mechanical energies. The energy contributions should be constructed from terms that obey Fermionic quantum mechanics. For example there should be no role for the *classical* electrostatic interactions associated with the *quantum* density.

a)Electronic mail: prhorn@berkeley.edu
b)Electronic mail: mhg@cchem.berkeley.edu

6. Continuous. The energy contributions should be continuous functions of the nuclear coordinates if the overall intermolecular interaction energy is continuous.

7. Computationally feasible. The computational cost for evaluation of each term should not be significantly greater than the direct evaluation of the entire intermolecular interaction.

8. Variational. To ensure validity in both weak and strong interaction regimes, the energy contributions should be defined as constrained variations[2–4] relative to an unconstrained calculation.

This work will focus on the construction of a definition for the polarization contribution to the interaction energy satisfying all of the above criteria but most notably the second two points, basis type independence and a non-trivial basis set limit.

There are many schemes for analyzing interaction energies that do not compute a polarization term with the meaning used in this work. The most common approach is to simply treat these two forms of relaxation, polarization and charge transfer, as inseparable, leading to the induction term in the traditional SAPT[5–9], the orbital term in Bickelhaupt-Baerends EDA[10–12], ETS[13–16], and the CI-singles based scheme of Reinhardt et al.[17], as well as the "polarization" term in LMO-EDA[18–20] and in the deformation density based scheme of Mandado and Hermida-Ramón[21].

Our view is that the polarization contribution to interactions is a physically meaningful quantity that is closely related to isolated monomer properties, despite not being uniquely defined in the overlapping regime. There are both variational and non-variational approaches to computing polarization energies. Among the non-variational schemes are those based on symmetry adapted perturbation theory (SAPT) that either bin excitations using a basis partitioning[22,23] to prohibit, or add potentials[24] to discourage, charge transfer contributions to the induction term. Another non-variational approach is natural energy decomposition analysis (NEDA)[25–29] in which the polarization contribution is largely determined by the natural bond orbital (NBO) method's ability or lack thereof to construct monomer Lewis structures from supersystem densities. Moreover, the NEDA polarization energy is computed as a difference involving the classical interaction of monomer densities.

The pioneering Kitaura-Morokuma (K-M) EDA[30–32] can be seen as the progenitor of variational EDAs, although it has the disadvantage that the energies used to define the polarization contribution do not correspond to the expectation values of valid wavefunctions. In much the same vein, the PIEDA[33,34] and SCCCMS-based[35,36] EDAs use FMO[37–40] and point charges, respectively, to optimize monomer wavefunctions in the presence of the classical electrostatic potentials of all other monomers, so the polarized state energy is also not the expectation value of an antisymmetric wavefunction. The CAFI[41] method also employs FMO to relax monomer wavefunctions but then uses a basis partitioning of CI-singles to investigate the additional polarization contributions that arise together with charge transfer . A slightly different approach to polarization is taken by the CSOV[42] and RVS[32,43] schemes in which the intermediate variational solutions come from the removal of certain orbital rotations in the optimization based on the monomer attribution of orbitals. The wavefunctions in these two methods are valid; however, subsystems are not able to relax simultaneously in contrast to the KM and related polarization schemes.

A novel method for the calculation of polarization energies is the constrained DFT approach of Wu[3,4], which constructs a polarized wavefunction by imposing a real-space population constraint. One advantage of this variational approach is that it circumvents the partitioning of basis functions among monomers that can be problematic for other methods; however, this method is not without its drawbacks, discussed at length later. We also mention that Řezáč and de la Lande[45] have recently used a similar constraint to isolate charge transfer contributions to the interaction energy.

A fairly common approach to obtaining a variational polarization energy is to solve for a polarized state using SCF for molecular interactions (SCF-MI) SCFMI[46,47], which both produces a valid wavefunction through constraints and allows for the simultaneous relaxation of all species. SCFMI polarization is a component of several EDA schemes including the block-localized wave function (BLW)-EDA[48–51] and the absolutely localized MO (ALMO)-EDA[2,52–54] schemes and the method of De Silva and Korchowiec[55]. We also note that the approach of Yamada and Koga[56] likewise uses SCF-MI to compute polarization energies; however, unlike the other three methods, the subspaces used are based on NBOs with the aim of investigating intramolecular interactions.

In the SCFMI-based schemes[2,48–55], the polarized state is obtained by the minimization of the single

determinant electronic energy of a collection of fragments with the constraint that the AO-to-MO coefficient matrix is fragment-blocked with an integer number of electrons assigned to each fragment. The polarization energy lowering is defined as the difference between the energy of this constrained solution and that of the frozen orbital density matrix, which is the projector into the span of the occupied orbitals of the fragments computed in isolation within their subspaces. The parameters for on-fragment-subspace orbital mixings are the degrees of freedom in the constrained optimization problem. These intra-subspace occupied-virtual rotations are seen as the polarization of each fragment, an interpretation that is reinforced by the fact that displacements on this constrained surface preserve fragment populations by the Mulliken definition[53,57]. Unlike in the KM polarization scheme, SCFMI polarization both recognizes and tries to relieve the increased kinetic energy that is a consequence of overlapping fragment occupied subspaces. The remaining inter-subspace rotations that lead to the optimal unconstrained determinant are identified as charge transfer in character because they do allow for changes in fragment populations by the Mulliken definition. The interpretation of the partitioned singles is simple and intuitive provided that the fragment subspaces which delimit intra- from inter-fragment mixings are in fact meaningful.

The definition of the polarization energy lowering in the SCFMI-based EDA schemes has two major weaknesses. The first is that the definitions for the fragment subspaces which determine the degrees of freedom in the variational energy calculation are intrinsically tied to the use of an atom-centered basis set. This means that standard SCF-MI is not applicable to calculations involving plane-wave basis sets among others. The second weakness is the assumption that the subspaces constructed from these AO functions are fragment-ascribable. In the limit that each atom is given a complete basis set, the fragment subspaces become linearly-dependent, and the subspace rotation constraint is effectively removed so that the SCFMI energy is equal to the full SCF energy. Hence the charge transfer contribution to the interaction becomes zero, a trivial basis set limit. This lack of a meaningful basis set limit for the SCFMI-based polarization term has been discussed by several authors[24,58,59].

Recently[60], an approximate lower bound for the polarization contribution was computed by the same constrained optimization but using orthogonal fragment subspaces of minimal rank designed to compactly describe intra-fragment orbital relaxations.
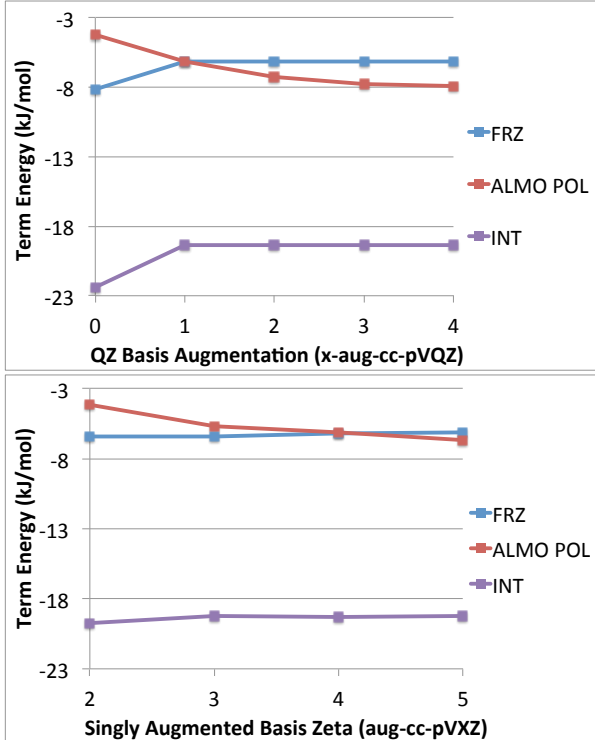

FIG. 1: Basis set convergence of some ALMO-EDA energy terms for the aug-cc-pVQZ/B3LYP optimized water dimer with an intermolecular distance of R_{O-H} = 1.96Å. The upper panel shows the effect of adding diffuse functions, while the lower panel shows the effect of increasing the cardinal number, X.

The upper bound was taken as the SCFMI-based polarization energy, which is clearly valid at the basis set limit and also very likely true for some of the larger common basis sets. Figure 1 demonstrates the poor basis set convergence of the polarization energy lowering in the original ALMO-EDA scheme compared to the much more quickly converged frozen and total interaction energies as a function of both basis set augmentation and basis set zeta. In practice (e.g. in using the ALMO-EDA or the BLW-EDA), the restriction to AO basis sets was simply an accepted limitation, and the lack of a useful basis set limit was tempered by the use of basis sets with function spaces that were largely fragment-ascribable (e.g. typically no larger than aug-cc-pVTZ). It is the goal of this work to overcome these weaknesses in the original definition of the polarization energy lowering in the SCFMI-based schemes by constructing new fragment subspaces.

The remainder of this paper is organized as follows. The theory, Sec. II, is based on defining "frag-

ment electric-field response functions" (FERFs) for each fragment, which form an appropriate basis for describing inductive effects. The FERFs can exactly (in a sense to be discussed) capture the response of an isolated fragment to weak electric fields. One FERF per occupied orbital is required for each independent component of a weak applied field. Thus there are 3 FERFs per occupied orbital for thee dipole (D) responses to a uniform field, 5 for the quadrupole (Q) responses to a field gradient, 7 for octupole (O) responses, etc. The polarization models we explore involve the use of D, DQ, or DQO sets of FERFs. The FERFs can be used directly as a basis for polarization, in which case they are non-orthogonal from one fragment to the next, and we will refer to such models as nD, nDQ, and nDQO. Alternatively, we next define orthogonalized FERFs, which give rise to the oD, oDQ, and oDQO models, using an importance-weighted orthogonalization that allows the FERFs that contribute most to polarization to be least distorted. Next, the interpretation of the SCFMI equations is re-evaluated in terms of orbital rotations, leading to an important distinction between some variational polarization schemes.

We then turn to the results of test calculations assessing the various FERF models on polarization contributions to a range of model intermolecular interactions. Vastly improved basis set convergence characteristics are found relative to the standard ALMO polarization model. We assess the differences in polarization energies predicted by the non-orthogonal and orthogonal models. The paper concludes with our recommendations for the use of these models, as well as some discussion of their merits relative to existing variational treatments of polarization in EDAs.

II. THEORY

General notation in this work is as follows: subspace indices: capital Roman $X, Y...$; AO and subspace basis indices: lower case Greek μ, $\nu...$; virtual MO indices: $a, b...$; occupied MO indices: $i, j...$; generic MO indices: $r, s.....$ This work considers non-orthogonal subspaces and thus makes considerable use of tensors with both covariant (subscript) and contravariant (superscript) indices.[61] Dots are used as placeholders for clear index ordering in quantities that have both covariant and contravariant indices. For instance, the matrix $\mathbf{C}$ with matrix elements $C^{X\mu\,\bullet}_{\bullet\,Yr}$ has rows corresponding to contravariant basis vectors associated with subspace X and columns

corresponding to covariant molecular orbitals associated with subspace Y, both occupied and virtual. For simplicity, matrices are generally given in spin-orbital notation, which permits simplification to any of the standard spin cases, such as either restricted or unrestricted. Exceptions will explicitly include a spin index as a subscript, as in $\mathbf{C}_\alpha$. Further notation will be introduced as needed.

A. Electric-Field Response Functions to Define Polarization Subspaces of Isolated Fragments

The role of the fragment polarization subspaces is to separate rotations that are polarization-like from those that are charge-transfer-like. An unambiguous distinction between the two only exists in the non-overlapping, well-separated, weak-field regime where charge-transfer is zero because of the lack of overlap but polarization is non-zero because of the presence of a field. In this limit, other fragments are well approximated by low-order multipole expansions, and polarization is the response to this multipole field, which, for single-determinant methods, is merely a matrix of occupied-virtual rotations.

It is preferable to consider polarization spaces that are inherent to the molecule such that they can be computed for the fragment in isolation with a sufficiently complete basis of any type. The first essential (and trivial) component of this space is the span of the occupied orbitals of the isolated fragment. The remaining vectors must come from the fragment's virtual subspace, and it is necessary to include some portion of this space in order that the given fragment is able to relax in the presence of other perturbing species.

In order to select supersystem-independent virtual functions, we consider fragment responses to general weak fields, field gradients, and so forth such that the fragment is able to respond to the presence of some other arbitrary, well-separated fragment. This will ensure that the correct asymptotic polarization behavior is recovered to sufficient accuracy. These orbital responses are exactly those computed in the calculation of dipole, quadrupole and higher polarizabilities, which are the second derivatives of the electronic energy with respect to field perturbations.

Denoting derivatives with superscripts, the orbital response (of a fragment) to the field component F_μ is Δ^μ. It is the solution to the following (coupled perturbed SCF (CPSCF)) linear equations obtained by differentiating the zero field SCF stationarity condition, $E^\Delta = 0$, with respect to the field component F_μ, which couples to the molecule by the multipole

moment matrix M_μ in the core hamiltonian, h:

$$E^{\Delta\Delta} \cdot \Delta^\mu = -E^{\Delta h} \cdot h^\mu \qquad \text{(II.1)}$$

$$E^{\Delta h} \cdot h^\mu \equiv \frac{\partial^2 E}{\partial \Delta^{ai} \partial h_{\lambda\sigma}} (h^\mu)_{\lambda\sigma} = 2(M_\mu)_{ai} \qquad \text{(II.2)}$$

$E^{\Delta\Delta}$ is the usual SCF orbital Hessian. In this work, the equation is solved for all RHS simultaneously using conjugate gradient preconditioned with the easily inverted $E^P \cdot P^{\Delta\Delta}$ portion of the Hessian. The fragment center of mass is taken as the origin for computing the cartesian multipole matrices, which are then transformed to the real spherical harmonic multipole matrices[62] appearing in the RHS.

The fragment orbital response matrix, Δ^μ, for a given field component, $F_\mu = F_x, F_y, F_z, \frac{\partial F_x}{\partial z}, \frac{\partial F_y}{\partial z}$, etc., which couples through the multipole moment matrix $M_\mu = \mu_x, \mu_y, \mu_z, Q_{xz}, Q_{yz}$, etc., is in general dense, describing the mixings of all occupied orbitals with all virtual orbitals. Singular Value Decomposition (SVD) of these amplitudes expressed in an orthogonal basis for a specific spin (we consider only the restricted closed-shell and unrestricted cases in this work),

$$(\Delta^\mu)_{ai} = (L_\mu)_{ab}(d_\mu)_{bj}(R_\mu^T)_{ji}, \qquad \text{(II.3)}$$

yields a unitary transformation of the virtual orbitals, $(L_\mu)_{ab}$. This transformation allows for the description of the orbital response in terms of only $\min(O, V)$ virtual orbitals, which are the fragment electric-field response functions (FERFs) for field component μ:

$$(V_\mu)^\nu_{\bullet\,b}{}^\bullet = C^\nu_{\bullet\,a}{}^\bullet (L_\mu)_{ab} \qquad \text{(II.4)}$$

FERFs are only defined for positive singular values, $(d_\mu)_{bj} \neq 0$. For basis sets that are appropriate for the calculation of polarizabilities (discussed at length later), the number of fragment virtual orbitals is considerably larger than the number of fragment occupied orbitals, and the subspace spanned by the FERFs is a small subset of the total virtual space. The number of FERFs is no larger than one FERF per considered field component per occupied orbital. Within this subspace, the response of the fragment to a weak field component of the given type is described exactly.

In this work, we consider three non-orthogonal FERF models for the polarization subspace for each fragment, A. First, the non-orthogonal dipole type, nD:

$$\mathbf{R^{nD}_{POL,A}} = \mathbf{P_A} \oplus \mathbf{span}\{\mathbf{V}_{\mu_x}, \mathbf{V}_{\mu_y}, \mathbf{V}_{\mu_z}\} \qquad \text{(II.5)}$$

Second, the non-orthogonal dipole plus quadrupole type, nDQ (using spherical harmonic indices):

$$\mathbf{R^{nDQ}_{POL,A}} = \mathbf{span}\{ \quad \mathbf{R^{nD}_{POL,A}}, \mathbf{V}_{\mathbf{Q_{2,-2}}}, \quad \text{(II.6)}$$
$$\mathbf{V}_{\mathbf{Q_{2,-1}}}, \mathbf{V}_{\mathbf{Q_{2,0}}}, \mathbf{V}_{\mathbf{Q_{2,1}}}, \mathbf{V}_{\mathbf{Q_{2,2}}}\}$$

Third and most demanding, the non-orthogonal dipole plus quadrupole plus octupole type, nDQO:

$$\mathbf{R^{nDQO}_{POL,A}} = \mathbf{span}\{ \quad \mathbf{R^{nDQ}_{POL,A}}, \mathbf{V}_{\mathbf{O_{3,-3}}}, \quad \text{(II.7)}$$
$$\mathbf{V}_{\mathbf{O_{3,-2}}}, \mathbf{V}_{\mathbf{O_{3,-1}}}, \mathbf{V}_{\mathbf{O_{3,0}}},$$
$$\mathbf{V}_{\mathbf{O_{3,1}}}, \mathbf{V}_{\mathbf{O_{3,2}}}, \mathbf{V}_{\mathbf{O_{3,3}}}\}$$

It is clearly possible to continue this series of models, but arguments will be made for the preferred truncation later, based on test calculations. For spin unrestricted calculations, alpha and beta polarization subspaces of these types will in general be different. No reference has been made to atom-tagged AO functions in these FERF models, and the fragment SCF and CPSCF equations can be solved in an appropriately complete basis of any type.

B. Constrained Solutions for General Fragment Spans

Given vectors, $G^\mu_{\bullet\,A\lambda}{}^\bullet$, for each fragment, A, spanning the fragment's polarization subspace, as defined by the projector $\mathbf{R_{POL,A}}$, one can obtain the polarized (SCFMI) determinant by solving one of the following slightly generalized non-linear eigenvalue problems for each fragment[46,47] and for each spin. In the equations below, the subscript S denotes the formulation of Stoll[46]:

$$[\mathbf{G}^T(\mathbf{1} - \mathbf{SP} + \mathbf{SP}_S^A)\mathbf{F} \qquad \text{(II.8)}$$
$$\times (\mathbf{1} - \mathbf{PS} + \mathbf{P}_S^A\mathbf{S})\mathbf{G}]_{AA}\mathbf{C}_A$$
$$= [\mathbf{G}^T\mathbf{SG}]_{AA}\mathbf{C}_A\epsilon_A$$

$$(P_S^A)^{\mu\nu} = \sum_Z G^\mu_{\bullet\,Z\lambda}{}^\bullet (T_Z)^{Z\lambda\,\bullet}_{\bullet\,Zj} \qquad \text{(II.9)}$$
$$\times \left((\sigma_{OO})^{-1}\right)^{ZjAi} (T_A^T)^{\bullet\,A\sigma}_{Ai\,\bullet}(G^T)^{\bullet\,\nu}_{A\sigma\,\bullet}$$

and the subscript G is used to denote the Gianinetti[47] approach.

$$[\mathbf{G}^T(\mathbf{1} - \mathbf{SP} + \mathbf{SP}_G^A)\mathbf{F} \qquad \text{(II.10)}$$
$$\times (\mathbf{1} - \mathbf{PS} + \mathbf{P}_G^A\mathbf{S})\mathbf{G}]_{AA}\mathbf{C}_A$$
$$= [\mathbf{G}^T(\mathbf{S} - \mathbf{SPS} + \mathbf{SP}_G^A\mathbf{S})\mathbf{G}]_{AA}\mathbf{C}_A\epsilon_A$$

$$(P_G^A)^{\mu\nu} = \sum_{YZ} G^{\mu\,\bullet}_{\,\bullet\,Z\lambda}(T_Z)^{Z\lambda\,\bullet}_{\quad\bullet\,Zj} \qquad \text{(II.11)}$$

$$\times \left((\sigma_{OO})^{-1}\right)^{ZjAi}\left((\sigma_{OO})^{-1}\right)^{AiYk}$$

$$\times (T_Y^T)^{\,\bullet\,Y\sigma}_{Yk\,\bullet}(G^T)^{\,\bullet\,\nu}_{Y\sigma\,\bullet}$$

In the above equations, the one-particle density matrix $\mathbf{P}$ is the projector into the occupied subspace,

$$\mathbf{P} = \sum_{XY} \mathbf{G}\mathbf{T}_X\left(\boldsymbol{\sigma}_{OO}\right)^{-1}\mathbf{T}_Y^T\mathbf{G}^T \qquad \text{(II.12)}$$

$$(\boldsymbol{\sigma}_{OO})_{XY} = \mathbf{T}_X^T\boldsymbol{\gamma}\mathbf{T}_Y \qquad \text{(II.13)}$$

$$\boldsymbol{\gamma} = \mathbf{G}^T\mathbf{S}\mathbf{G} \qquad \text{(II.14)}$$

and the Fock matrix, $\mathbf{F}$, is the derivative of the energy with respect to this occupied subspace projector:

$$F_{\mu\nu} = \frac{\partial E}{\partial P^{\mu\nu}} \qquad \text{(II.15)}$$

$\mathbf{C}_A$ are the fragment coefficient matrices for the covariant molecular orbitals in the contravariant $\mathbf{G}$ basis with the occupied subset of these vectors denoted by $\mathbf{T}$ and the virtual subset denoted by $\mathbf{V}$. The $\mathbf{C}_A$ can be collected into a global matrix, $\mathbf{C}$, which is subspace-block-diagonal, analogous to the coefficient matrices in the original SCFMI scheme (for which $\mathbf{G}$, the matrix of subspace vectors in terms of the AO basis, is simply the identity matrix).

The projected Fock operators in the LHS of equations (II.8) and (II.10) can be extrapolated and diagonalized using the DIIS[63] algorithm with the following error vector for each fragment, A:

$$\mathbf{Err}_{AA} = \boldsymbol{\gamma}_{AA}\left[\boldsymbol{\gamma}^{-1}\mathbf{G}^T\mathbf{S}\mathbf{P}\mathbf{F}\left(\mathbf{P}\mathbf{S}-\mathbf{1}\right)\mathbf{G}\right]_{AA}$$
$$- \text{Transpose} \qquad \text{(II.16)}$$

Alternatively, one can zero the gradient of the energy with respect to intra-subspace orbital rotation parameters, $\{\boldsymbol{\Delta}_A\}$ (which can also be collected into a global fragment-diagonal matrix, $\boldsymbol{\Delta}$):

$$\mathbf{C}_A \leftarrow \mathbf{C}_A\mathbf{U}_A = \mathbf{C}_A\,\exp\left(\boldsymbol{\Delta}_A - \boldsymbol{\Delta}_A^T\right) \qquad \text{(II.17)}$$

$$C^{A\mu\,\bullet}_{\,\bullet\,As} \leftarrow C^{A\mu\,\bullet}_{\,\bullet\,Ar}\,\sigma^{A\bar{r}A\bar{t}}_{AA}[\qquad \text{(II.18)}$$
$$+ \sigma_{AtAs} + \Delta_{AtAs} - \Delta_{AsAt}$$
$$+ \tfrac{1}{2}\Delta_{AtAu}\sigma^{A\bar{u}A\bar{v}}_{AA}\Delta_{AvAs} - \tfrac{1}{2}\Delta_{AtAu}\sigma^{A\bar{u}A\bar{v}}_{AA}\Delta_{AsAv}$$
$$- \tfrac{1}{2}\Delta_{AuAt}\sigma^{A\bar{u}A\bar{v}}_{AA}\Delta_{AvAs} + \tfrac{1}{2}\Delta_{AuAt}\sigma^{A\bar{u}A\bar{v}}_{AA}\Delta_{AsAv}$$
$$+ O\left(\boldsymbol{\Delta}^3\right)]$$

$$\left.\frac{\partial E}{\partial \Delta_{ApAq}}\right|_{\boldsymbol{\Delta}=0} = \left.\frac{\partial E}{\partial P^{\mu\nu}}\frac{\partial P^{\mu\nu}}{\partial \Delta_{ApAq}}\right|_{\boldsymbol{\Delta}=0} \qquad \text{(II.19)}$$
$$= 2[\delta_r^p\delta_i^q - \delta_i^p\delta_r^q]$$

$$\times \left[\sum_Z (\boldsymbol{\sigma}_{OO})^{-1}\mathbf{T}_Z^T\mathbf{G}^T\mathbf{F}\left(\mathbf{I}-\mathbf{P}\mathbf{S}\right)\mathbf{G}\mathbf{C}_A(\boldsymbol{\sigma}_{AA})^{-1}\right]^{AiA\bar{r}}$$

for each subspace, A with one's non-linear solver of choice. Contravariant indices with bars ($A\bar{p}$) indicate that the index is not globally contravariant but rather contravariant with respect to the covariant metric for the given subspace (A). The gradient is subspace-blocked, and exponentiation of the corresponding displacements yields subspace-block-diagonal orthogonal (in the general non-orthogonal sense) orbital updates. We note that this gradient as written has occupied-occupied rotation dependence in addition to the usual occupied-virtual dependence if intra-subspace occupied-virtual orthogonality is not enforced (if the columns of $\mathbf{T}_A$ and $\mathbf{V}_A$ are not orthogonal). The subspace-block-diagonal vectors in $\mathbf{C}$, thus far only assumed to be intra-subspace linearly independent, can be chosen to be intra-subspace orthonormal ($\boldsymbol{\sigma}_{AA}=\mathbf{I}$) without loss of generality, resulting in slightly simpler expressions and algorithms.

In several calculations in this work, a quasi-Newton algorithm incorporating an approximate inverse Hessian (preconditioned L-BFGS)[64,65] and the Newton-Raphson algorithm itself were employed to solve the SCFMI problem to obtain the polarized determinant. The Hessian for the SCFMI problem has been presented previously for different variables[46], and it is presented without the assumption of intra-subspace orthogonality for the orbital rotation parameters used in this work in the appendix (C.2) along with relevant intermediates. Additionally, in Appendix D we include a detailed discussion of our preconditioning strategy.

C. Orthogonal Polarization Subspaces

We next consider the construction of orthogonal fragment polarization subspaces that are based on the non-orthogonal subspaces discussed above. Orthogonalized models are a way to explore approximate bounds on the magnitude of polarization energy lowerings. They may be particularly appealing to those who, for one reason or another, consider carrying a metric to be heretical[66] and prefer instead the onus of the caveats that we now enumerate:

1. The construction of orthogonal projectors from non-orthogonal spans is not unique, and while it is possible to form these orthogonal subspaces in a way that is in some sense optimal, the corresponding merit function will always be arbitrary.

2. Orthogonal subspaces ascribed to fragments are not appropriate spans for describing the electronic structure of those fragments in isolation (except in the uninteresting limit where no orthogonalization is required).

3. If the number of degrees of freedom in the SCFMI problem is unchanged, then, while the orthogonal subspaces may seem more restrictive, all that can be said is that the degrees of freedom are *different.* SCFMI energies computed with arbitrary orthogonal subspaces therefore have no variational guarantee to be an upper bound to the energy computed with non-orthogonal subspaces of the same rank.

4. As an extreme example, the *exact* MO's (after localization) can be partitioned into orthogonal SCFMI subspaces such that the exact SCF energy could be obtained from the solution of the (albeit poorly) constrained SCFMI problem.

To avoid such pitfalls, we insist that the vectors after orthogonalization be justifiably tagged to a subspace. From the previous section, we already have a method to ascribe all polarization-relevant vectors in the system to *non-orthogonal* SCFMI subspaces. Hence an appropriately weighted symmetric orthogonalization[67] (II.20), which preserves fragment tagging by pairing each non-orthogonal vector with a single orthogonal counterpart, is a natural choice.

$$G^{\mu\,\bullet}_{\bullet\,A\lambda} \leftarrow \sum_B G^{\mu\,\bullet}_{\bullet\,B\rho} C^{B\rho\,\bullet}_{\bullet\,Br} \qquad \text{(II.20)}$$
$$\times \left[\mathbf{W} \left(\mathbf{W}\boldsymbol{\sigma}\mathbf{W} \right)^{-\frac{1}{2}} \right]^{Br\,\bullet}_{\bullet\,As}$$

For systems like water interacting with a sodium cation, minimal CT is expected, but inappropriate construction of the orthogonal subspaces could inhibit the water molecule from properly polarizing in response to the presence of the cation. The result would be an unduly large CT contribution to the interaction. To allow adequate water polarization with orthogonal subspaces, we could preserve the important water FERFs unmodified and orthogonalize the less vital sodium FERFs against them. To bring about this outcome in a black-box way, we will construct the weights such that FERFs deemed more important for polarization are given larger weights so that they are least deformed by orthogonalization. The resulting weights should create the greatest lower bound on the stabilization energy from polarization. Non-orthogonal FERFs contain exactly the degrees of freedom necessary for the fragment to relax in the presence of weak fields, and any modification of the FERF subspaces (such as orthogonalization) should impede this relaxation.

Orthogonalization necessitates that functions in one domain develop "tails" in other domains. Some systems could exploit such degrees of freedom during the polarization stage of the calculation to bring about delocalization of charge that would have otherwise occurred during the CT portion of the corresponding non-orthogonal calculation. This should only occur when there is a physical motivation for such mixings. For systems with very little CT, such as H_2O-Na^+, this premature delocalization of charge should only occur to a negligible extent even if the orthogonal subspace construction permits it. The question of whether this consequence of orthogonalization is problematic (giving overly large polarization energies when CT is important), must be assessed by test calculations.

In this work, the weight matrix is chosen to be diagonal with values between 1 and 100 to avoid poor conditioning of $\mathbf{W}\boldsymbol{\sigma}\mathbf{W}$ from an excessively large range of weights. The first step in generating the weights is the construction of intra-subspace mixing amplitudes, $(\mathbf{X}_A)_{VO}$, by considering the rotations necessary to solve the Stoll[46] equation (II.8) for each fragment and unique spin with fixed frozen orbital density and corresponding Fock operators[68,69].

$$(\mathbf{F}_A)_{VO} + (\mathbf{F}_A)_{VV}(\mathbf{X}_A)_{VO} - (\mathbf{X}_A)_{VO}(\mathbf{F}_A)_{OO} - (\mathbf{X}_A)_{VO}(\mathbf{F}_A)_{OV}(\mathbf{X}_A)_{VO} = (\mathbf{0}_A)_{VO} \qquad \text{(II.21)}$$

$$(\mathbf{F}_A)_{OO} = \left[\sum_{YZ} (\boldsymbol{\sigma}_{OO})^{-1} \mathbf{T}_Y^T \mathbf{G}^T \mathbf{F_G} \mathbf{T}_Z (\boldsymbol{\sigma}_{OO})^{-1} \right]_{AA} \qquad \text{(II.22)}$$

$$(\mathbf{F}_A)_{VO} = \left[\sum_Z \mathbf{V}_A^T \mathbf{G}^T \left(\mathbf{1} - \mathbf{SP} \right) \mathbf{FGT}_Z (\boldsymbol{\sigma}_{OO})^{-1} \right]_{AA} \tag{II.23}$$

$$(\mathbf{F}_A)_{VV} = \left[\mathbf{V}_A^T \mathbf{G}^T \left(\mathbf{1} - \mathbf{SP} \right) \mathbf{F} \left(\mathbf{1} - \mathbf{PS} \right) \mathbf{GV}_A \right]_{AA} \tag{II.24}$$

In practice, the projected virtuals used for the amplitudes are on-fragment orthogonalized to remove any virtual vectors lying entirely in the occupied subspace. Singular value decomposition (SVD) of the amplitudes for each fragment (II.25) yields a single scalar for each orbital that describes, after transformation by the eigenvectors, the importance of that orbital for intra-subspace relaxations.

$$(\mathbf{X}_A)_{VO} = \mathbf{L}_A \mathbf{x}_A \mathbf{R}_A^T \tag{II.25}$$

In general, the amplitudes have different row and column dimensions, leaving some vectors with a weight of identically zero. In order to give all vectors non-zero weights, the non-zero singular values across all fragments are uniformly scaled such that the smallest non-zero singular value is 1. The vectors with exactly zero singular values are then given weight 1 such that they have the same importance as the least important vector with non-zero singular value. The weights are then forced to be in the range 1 to 100 while still preserving importance ordering by taking the weights associated with all vectors to the same power.

With the weights in hand, application of (II.20) is straightforward. This process is performed first for the occupied orbitals of the supersystem, providing a new definition of the occupied subspace of each fragment. The process is then repeated for the globally projected and intra-subspace orthonormalized FERFs determined by the field responses, taking into account the newly defined, orthogonal fragment occupied subspaces in the construction of the amplitudes. The projection of virtual FERFs into the orthogonal complement of the global occupied subspace allows for the construction of orthogonal fragment subspaces without changing the supersystem occupied subspace projector from that of the frozen orbitals.

Because the occupied orbitals used to compute the weights for the virtual subspaces weighted symmetric orthogonalization are orthogonal, the linearized version of the amplitude equation (II.21) obtained by deleting the term quadratic in $(\mathbf{X}_A)_{VO}$ yields the same equation for the amplitudes used previously to construct a compact set of orthogonal functions for

polarization, polMOs[60]. While the intra-subspace amplitudes are determined using the same expressions, there are important differences between the current procedure and that which defines the polMOs. Notably, in the polMO procedure, amplitudes are computed using fragment-tagged occupied and virtual vectors with a collective span equal to that of all atom-centered AO basis functions on the fragment. Moreover, only eigenvectors with non-zero singular values are included in the weighted symmetric orthogonalization, and the singular values associated with these vectors are used directly as the weights. Thus, the treatment of weights and the spans that are considered for orthogonalization are different. Furthermore, the polMO procedure relies on atom-centered basis functions to define fragment subspaces for amplitude construction.

The variational polarization of a system with orthogonal fragment subspaces can be performed using a simplified version of the Stoll[46] and Gianinetti[47] eigenvalue equations as described previously[60]. Alternatively, one can use the above gradient and Hessian equations (Appendix D) for Newton or quasi-Newton methods with $\boldsymbol{\gamma} = \boldsymbol{\sigma} = \mathbf{I}$.

D. Delineation Between Polarization and Charge Transfer

One consequence of using both the general, non-orthogonal and orthogonalized versions of the FERFs is that fragment populations as computed by the traditional AO Mulliken scheme can change during self-consistent polarization. This was not the case for the original, atom-centered AO basis scheme[53,57]. However, charges are preserved by a modified Mulliken definition where instead of tracing fragment-diagonal blocks of the contravariant-covariant density matrix in the AO basis, one instead traces the contravariant-covariant density matrix in the basis of the columns of $\mathbf{G}$ defining the polarization subspace of each fragment. Again, the original SCFMI-based EDA result is recovered for $\mathbf{G} = \mathbf{I}$.

A notable special case occurs when non-orthogonal FERFs are computed using only the AO

functions from that fragment, which is the way they are later employed in production calculations. In this case, there is also no charge flow during polarization by the traditional Mulliken definition as the non-orthogonal FERF polarization subspaces are exact subsets of the original SCFMI polarization subspaces. Another special case arises when one of the orthogonal schemes is used. In this case, both the modified Mulliken and comparably modified Löwdin schemes will compute no inter-fragment charge flow during polarization.

The population conserving character of the SCFMI degrees of freedom by a modified Mulliken-like definition is the basis for the interpretation of the intra-subspace relaxations in the polarization step as excluding charge transfer interactions; however, the SCFMI-based schemes are not the only ones that can make this claim. The density-based EDA of Wu[3,4] likewise conserves fragment populations during the polarization stage of the calculation though by a real-space partitioning of charges. We shall show that the distinction between these two flavors of variational polarization goes well beyond the definition of the chosen population scheme. SCFMI-allowed rotations are not only population conserving but also what we will refer to as charge-flow-prohibiting. Charge-flow-prohibiting rotations are a subset of the population conserving rotations, all of which are allowed in Wu's constrained-DFT-based decomposition.

The remainder of this section is structured as follows. First, we will show in a more involved but instructive way that SCFMI rotations are population conserving. Next, we will introduce the full SCF degrees of freedom into the SCFMI objective function by the construction of linearly dependent subspaces and identify the form of displacements utilizing these additional degrees of freedom that are likewise population conserving. Finally, we will discuss the interpretation of these population conserving but not charge flow prohibiting displacements as they relate to polarization and charge transfer.

The population of a domain, A, by a generalized Mulliken definition is:

$$\text{Pop}_A = [\mathbf{S}\mathbf{P}_A\mathbf{S}]_{\mu\nu} P^{\mu\nu} \qquad (\text{II.26})$$

where we define:

$$P_A^{\lambda\sigma} = \sum_X M^{\lambda\,\bullet}_{\bullet\,A\tilde{\pi}} \mu^{A\tilde{\pi}X\tilde{\beta}} (M^T)^{\bullet\,\sigma}_{X\tilde{\beta}\,\bullet} \qquad (\text{II.27})$$

$$\mu_{A\tilde{\pi}X\tilde{\beta}} = (M^T)^{\bullet\,\lambda}_{A\tilde{\pi}\,\bullet} S_{\lambda\sigma} M^{\sigma\,\bullet}_{\bullet\,X\tilde{\beta}} \qquad (\text{II.28})$$

The usual AO Mulliken scheme is recovered with $\mathbf{M} = \mathbf{I}$. The operator $\hat{P}_A$ is neither a projector nor symmetric except when the columns of $\mathbf{M}$ are orthogonal. The change in the population of domain A due to SCFMI-like displacements, $\mathbf{D} = [\mathbf{D}_A, \mathbf{D}_B, ...]$, can be written as:

$$\Delta\text{Pop}_A = \sum_X \mathbf{D}_X \cdot \frac{\partial\text{Pop}_A}{\partial\boldsymbol{\Delta}_X}\bigg|_{\boldsymbol{\Delta}=\mathbf{0}} \qquad (\text{II.29})$$

$$+ \sum_{XY} \frac{1}{2}\mathbf{D}_X \cdot \frac{\partial^2\text{Pop}_A}{\partial\boldsymbol{\Delta}_X\partial\boldsymbol{\Delta}_Y}\bigg|_{\boldsymbol{\Delta}=\mathbf{0}} \cdot \mathbf{D}_Y + O(\mathbf{D}^3)$$

The first (E.1) and second (E.2) derivatives of populations with respect to the SCFMI parameters, $\boldsymbol{\Delta}_X$, can be found in the appendix along with the relevant intermediates. If $\mathbf{M} = \mathbf{G}$, corresponding to the modified Mulliken definition discussed above, it can be shown that both the population gradient and Hessian with respect to SCFMI rotations are zero (Appendix E), yielding by (II.29) constant populations through second order in SCFMI displacements.

We now construct linearly dependent SCFMI subspaces, $A', B', ...$, (the above equations do not require any particular relationship among the vectors $\mathbf{G}$ defining different subspaces beyond that it be possible to construct a nonsingular occupied subspace metric) such that each occupied orbital is able to mix with every other orbital, the full degrees of freedom in unconstrained SCF. The distinction is that, in the linearly dependent SCFMI case, independent displacements are made on a number of Grassmann manifolds equal to the number of subspaces instead of only one, and the difficulties associated with these redundant and less connected degrees of freedom are shifted into the objective function with variable occupied subspace metric.

$$span\{\mathbf{G}]_{A'}\} = span\{\mathbf{M}]_A, \mathbf{M}]_B, \mathbf{M}]_C, ...\} \quad (\text{II.30})$$

$$(C_{A'})^{\nu\,\bullet}_{\bullet\,A'r} = G^{\nu\,\bullet}_{\bullet\,A'\pi}(C_{A'})^{A'\pi\,\bullet}_{\bullet\,A'r} \qquad (\text{II.31})$$
$$= \sum_X M^{\nu\,\bullet}_{\bullet\,X\tilde{\rho}}(C_{A'})^{X\tilde{\rho}\,\bullet}_{\bullet\,A'r}$$

We have used the notation $\mathbf{X}]_Y$ to indicate the columns of the matrix $\mathbf{X}$ with label Y.

For the purposes of this discussion, we will consider a specific initial condition where the orbitals in each subspace are written as follows:

$$(C_{X'})^{\mu\,\bullet}_{\bullet\,Z\hat{s}} = \qquad (\text{II.32})$$
$$\left[\delta^\mu_\lambda - \left(\delta^\mu_\sigma - \delta^\mu_\sigma \delta^X_Z\right)\Phi^{\sigma\nu}_X S_{\nu\lambda}\right]$$
$$\times M^{\lambda\,\bullet}_{\bullet\,Z\tilde{\gamma}}(C_Z)^{Z\tilde{\gamma}\,\bullet}_{\bullet\,Zs}$$

$$\Phi_X^{\sigma\nu} = M^\sigma_{\bullet \, X\tilde{\alpha}} (\mu_{XX}^{-1})^{X\tilde{\alpha}X\tilde{\beta}} M^\nu_{\bullet \, X\tilde{\beta}}$$

The vectors $(C_Z)^{Z\tilde{\gamma} \bullet}_{\bullet \, Zs}$ span the same space as the columns $\mathbf{M}]_Z$ and are thus of the same form as the MOs for subspace Z in a $\mathbf{G} = \mathbf{M}$ SCFMI calculation. The hat notation, $Z\hat{s}$, in the coefficients, $(C_{X'})^\mu_{\bullet \, Z\hat{s}}$, has been introduced to carry along Mulliken-domain-based tags from the $\mathbf{G} = \mathbf{M}$ SCFMI subspace Z to the linearly dependent SCFMI subspace X'. The MOs in subspace X' are in general of the form (II.31), but the Mulliken-domain attribution of the columns of $(C_{\alpha,X'})^\mu_{\bullet \, X's}$ by (II.32) will allow us to identify the form and character of the new degrees of freedom in the linearly dependent SCFMI.

Vectors of the form $(C_{\alpha,X'})^\mu_{\bullet \, Z\hat{s}}$ are virtuals in linearly dependent SCFMI subspace X' if $X \neq Z$, and these vectors, by (II.32), are in the orthogonal complement of the $\mathbf{G} = \mathbf{M}$ SCFMI subspace X. This means that rotations involving the $(C_{X'})^\mu_{\bullet \, Z\hat{s}} (X \neq Z)$ are explicitly new degrees of freedom for linearly dependent subspace X' relative to those of X. A consequence of this choice is that the subspace metric for X', $\boldsymbol{\sigma}_{X'X'}$, and thus its inverse are block-diagonal:

$$(\sigma_{X'X'})_{X\hat{r}Z\hat{s}} = \delta_Z^X (\sigma_{X'X'})_{X\hat{r}X\hat{s}} \qquad \text{(II.33)}$$

Moreover, by (II.32), vectors previously in subspace X are duplicated in subspace X', which means that SCFMI subspaces X and X' can and do have all occupied vectors identical at our initial condition. This establishes the connection between primed and unprimed subspace counterparts, and their indices should be assumed to be coupled in expressions in which they both appear. We note that in order to maintain these Mulliken-based labels for general Mulliken subspaces, orthogonality of the MOs in each linearly dependent SCFMI subspace, X', is not assumed.

In this notation, the degrees of freedom in A' corresponding to those in A, all of which have already been shown to be population conserving, are of the form $(\Delta_{A'})_{A\hat{p}A\hat{q}}$, and because of the way in which the vectors spanning A' were constructed ((II.32) and (II.33)), they remain population conserving by (II.29) after introducing the new degrees of freedom (Appendix F). New variables are of the form $(\Delta_{A'})_{A\hat{i}B\hat{s}}$ because our parametrization has no virtual-virtual rotation dependence and because all occupied orbitals in A' at the initial condition have Mulliken-domain tag A. These new variables will be

referred to as delocalization degrees of freedom. It is important to note that vectors written $B\hat{i}$ in A' are virtual vectors for subspace A' despite the occupied index.

With the form of the new degrees of freedom identified and the old degrees of freedom verified to remain population conserving, it is clearly possible to write the change in population to second order in terms of delocalizing displacements (II.29) for a general, non-orthogonal Mulliken partitioning (Appendix F); however, such a cumbersome expression is not apt for the current purpose. To facilitate interpretation, we will analyze the case where the columns of $\mathbf{M}$ are orthogonal, and thus $\boldsymbol{\sigma}_{OO}$, $\boldsymbol{\sigma}_{XX}$, $\boldsymbol{\sigma}_{X'X'}$, and $\boldsymbol{\mu}$ are or can be chosen without loss of generality to be $\mathbf{I}$. In this case, the change in population to second order is:

$$\Delta\text{Pop}_A = \sum_{X'} \sum_{Z \neq X} \sum_{\hat{i}\hat{a}} [(D_{X'})_{X\hat{i}Z\hat{a}}]^2 [\delta_A^Z - \delta_A^X]$$

$$\text{(II.34)}$$

The displacements that zero (II.34) for all A are delocalizing but also population conserving for small displacements, and it is clear from this expression that there are many delocalizing rotations that produce no net change in populations through second order. If we consider a system with only two Mulliken domains, A and B, then by conservation of total population we need only satisfy:

$$0 = \sum_{\hat{i}\hat{a}} [(D_{B'})_{B\hat{i}A\hat{a}}]^2 - [(D_{A'})_{A\hat{i}B\hat{a}}]^2 \qquad \text{(II.35)}$$

and the physical interpretation is that charge flows from domain A into domain B, but an equal amount of charge flows from domain B into domain A.

We do not see these sorts of delocalizations as polarization in character but rather as contributing to the kinetic energy lowering associated with inter-fragment orbital or bonding interactions. We emphasize that methods that merely constrain populations like those based on constrained DFT allow all population conserving rotations including some of those that we have termed delocalizing. In SCFMI-based schemes, only charge-flow-prohibiting rotations contribute to polarization, and all delocalization degrees of freedom - population conserving though they may be - are treated collectively as charge transfer contributions.

An important class of systems that highlights the difference between the two approaches to polarization are those in which all fragments are equivalent by symmetry. Meaningful population schemes should respect the point group symmetry of the

system, as must the unconstrained density. Thus, if the fragments are all constrained to have the same charge, then schemes that allow all population conserving rotations must then yield identically zero "charge transfer" contribution! SCFMI-based schemes that only allow charge-flow-prohibiting rotations do not enforce this trivial solution for CT, although it may still be zero for other reasons. The case of high symmetry systems is merely an extreme example of complexes where the forward and back donation of electrons is not well described by their signed sum. Thus, this distinction between the two approaches is expected to be quite relevant beyond model systems.

We note that Misquitta[24] also discusses the imprecision of the label "CT" with a preference instead for the term delocalization. We agree with this interpretation; however, to avoid unnecessary confusion, we will continue to use the term charge transfer to describe the energy lowering associated with the delocalization degrees of freedom. Possible further decompositions along these lines within the CT term are beyond the scope of this work.

E. Treatment of Charge Transfer and Basis Set Superposition Error

With new schemes for polarization defined and the frozen energy unaltered, it remains to discuss the treatment of the final component of energy lowering, charge transfer, in light of these modifications. In this work we employ only the subtractive approach in which the charge transfer energy lowering is computed as the difference between the energy of the optimal subspace-rotation-constrained determinant and the fully optimized supersystem determinant, guaranteeing recovery of the total binding energy. Note that the tools developed for decomposing charge transfer interactions in the original ALMO[53] scheme are not directly applicable here if one seeks to recover the full binding energy or a perturbative approximation thereof because not all vectors in the supersystem have been assigned to a fragment. The development of modified approaches will be a focus of future work.

If isolated fragments are computed with only their respective AO basis sets, then there will be a nonzero basis set superposition error (BSSE) contribution to the interaction energy. BSSE was problematic for SCFMI-based EDA schemes previously because the diffuse basis sets required to make BSSE negligible had to be avoided to ensure that the polarization and CT terms remained meaningful.

With these new FERF schemes, creating fragment-ascribable subspaces is no longer an issue, and large basis sets that do not require BSSE corrections can be employed. For systems with many fragments, the ability to compute responses fragment by fragment (without using the global basis) is an immense computational advantage.

III. RESULTS AND DISCUSSION

A. Computational Details

Calculations in this work were performed with a development version of QChem[70,71], which was extensively modified to implement the non-orthogonal FERF (using fragment blocking) and orthgonalized FERF models for describing polarization. Because multiply augmented Dunning basis sets have not been defined for all of the elements used in this work, multiply augmented basis sets were constructed for all atoms systematically from Dunning[72,73] aug-cc-pVXZ basis sets by the addition of one primitive per angular momentum with an exponent half the size of the next smallest primitive exponent for that angular momentum. Multiply augmented functions used in this work are thus slightly less diffuse than those in parametrized basis sets; however, this allows for basis sets of larger rank to be used before encountering severe linear dependencies. Though the method can be used with any density functional, the B3LYP[74–76] functional is used throughout this work as it is in common use and its second functional derivatives are available to us. Additionally its deficiencies for intermolecular interactions relate to dispersion-dominated interactions, which are not of interest here. It should be noted that, for functionals with density-independent corrections (for example, dispersion-corrected functionals of the D2 or D3 type[77,78]), the binding energy associated with these corrections resides in the frozen orbital energy term. While the systems analyzed in this work are dimers, this method can treat a cluster of an arbitrary number of fragments either directly or by means of a many-body expansion of arbitrary order.

B. Assessment of Non-Orthogonal Fragment Electric Field Response Functions (FERFs)

The new methods for constructing the FERFs do not depend on the use of atom-centered basis functions. However, because our molecular electronic

structure code[70,71] is based on gaussian AOs, we do in fact employ these standard quantum chemistry basis sets to demonstrate basis set convergence and assess both behavior and feasibility of these models. We compute FERF spans using only the given fragment's AO functions and not the entire supersystem basis as the goal is to identify basis sets capable of describing both the ground state density as well as the field responses. Hence the FERF polarization energies are variationally guaranteed to be less than or equal in magnitude compared to the corresponding ALMO polarization energies.

Figure 2a shows the basis set convergence of the polarization energy of the original ALMO and the new non-orthogonal FERF models, for the water dimer. It is clear from Figure 2a that ALMO does not converge at all in the basis set sequences examined. By contrast, the new FERF-based models do converge towards basis set limits which are characteristic of each model. Whilst the nD model is clearly converged at the aTZ basis, larger basis sets are required to converge the higher order FERF models, particularly the nDQO model. For the smallest basis sets considered (e.g. TZ), the response schemes produce polarization energies that are quite similar to the ALMO result, primarily due to basis set deficiencies.

Some general observations about convergence of the FERF models can be made. For atoms, each multipole response order requires basis functions of one higher angular momentum relative to that of the highest momentum valence orbital (eg. p-orbitals allow s-orbitals to respond to a dipole field, and d-orbitals allow s-orbitals to respond to a quadrupole field). The analogous response pairs are less clear for molecular fragments where functions of higher angular momentum than an atom's valence are necessary to describe the chemical environment (i.e. d functions for the water molecule). However the behavior is analogous: referring again to Figure 2a, basis set convergence is achieved for nD at triple zeta, nDQ at quadruple zeta, and nDQO at quintuple zeta provided sufficiently diffuse functions are included.

Given the increasing difficulty in converging the nD, nDQ, and nDQO models with respect to basis set, it is preferable to use lower order models if they are qualitatively correct on approaching the non-overlapping regime. It is also clear from Figure 2a that the progression of FERF model subspaces to high multipole orders will eventually develop the flexibility and thus the problems of the ALMO model itself. For this reason also, we would like to choose the smallest FERF model that is capable of a correct description of long-range polarization.

To this end, we investigated the distance dependence of the polarization energy of the FERF models and the original ALMO scheme for the dissociation of the water dimer along the O-O coordinate (Figure 2b). The d-aug-cc-pVQZ basis was chosen because it is one of the smallest to display clear differences in polarization energies for all methods at R_e. The polarization energies all appear fairly similar past R_e and at first seem only to distinguish themselves at compressed distances where there is no a priori correct answer.

To further differentiate the models, we investigated the polynomial decay (Figure 3) that they yield for the polarization energy for the water dimer (asymptotically an R^{-6} dipole induced-dipole interaction). Figure 3a shows the polynomial decay in the overlapping regime, highlighting again the considerable differences in the models for short intermolecular distances. In the long-range (Figure 3b), all methods approach but do not reach the R^{-6} limit before numerical difficulties set in at large R_{OO}. Evidently higher order polarization terms (e.g. quadrupole-induced dipole) are not yet negligible at these separations. Nonetheless, the interfragment overlaps are small enough that we can view the most variationally flexible method, ALMO, as the correct answer. This is because, in the long range, charge transfer is zero, and, because our model chemistry lacks a description of long-range electron correlation, all binding beyond the permanent electrostatic interaction (described by the ALMO frozen energy term) is the exact polarization energy of the classical polarization theory within this model chemistry. In the case of a model chemistry that does include long-range electron correlation, such as in the case of the exact exchange-correlation functional itself, deviations from the classical polarization theory will arise due to ALMO's effective partitioning of the polarization-dispersion cross terms of the classical polarization theory into separate contributions. A thorough treatment of inter-fragment electron correlation contributions to binding within the framework of SCFMI-based EDA is beyond the scope of this work but will be addressed in a future publication. The inability of a FERF model to reproduce the exact ALMO result in the long range thus indicates that it is inadequate for the description of polarization in the molecular field, which is more complicated than a simple field or field gradient.

Based on Figure 3b, the distance dependence of the polarization energy as computed by the nDQ and nDQO models is the same as that of ALMO while nD, which has the least variational flexibility to describe polarization, behaves qualitatively differ-
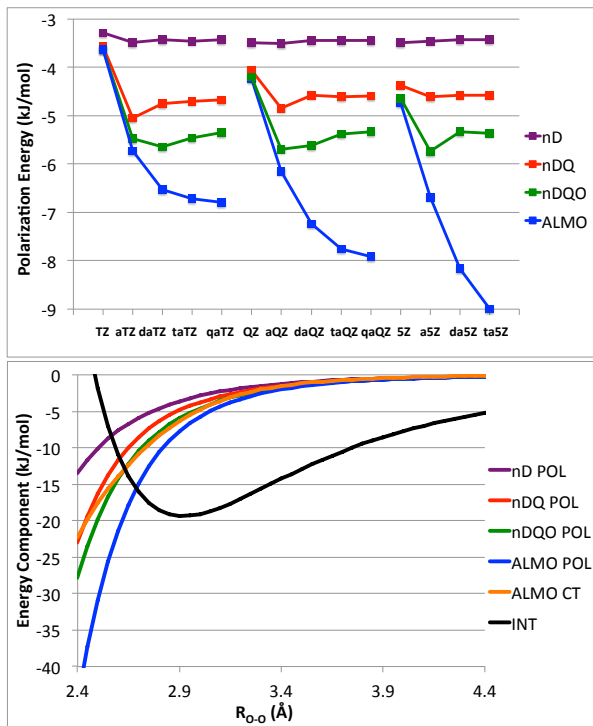
FIG. 2: Basis set convergence (a) at R_e ($R_{O-H} = 1.96$ Å) and distance dependence (b) of the polarization energy computed by ALMO and FERF models for the B3LYP/aug-cc-pVQZ optimized water dimer. The upper panel, (a), shows that the FERF polarization energies converge to useful basis set limits, which the ALMO model cannot achieve. The lower panel, (b), shows the distance dependence of B3LYP/d-aug-cc-pVQZ ALMO and FERF polarization energies, the total interaction energy (INT) and the ALMO charge transfer (CT) energy for rigid dissociation along the O-O coordinate. While similar at R_e and beyond, the polarization models produce considerably different results at compressed geometries.
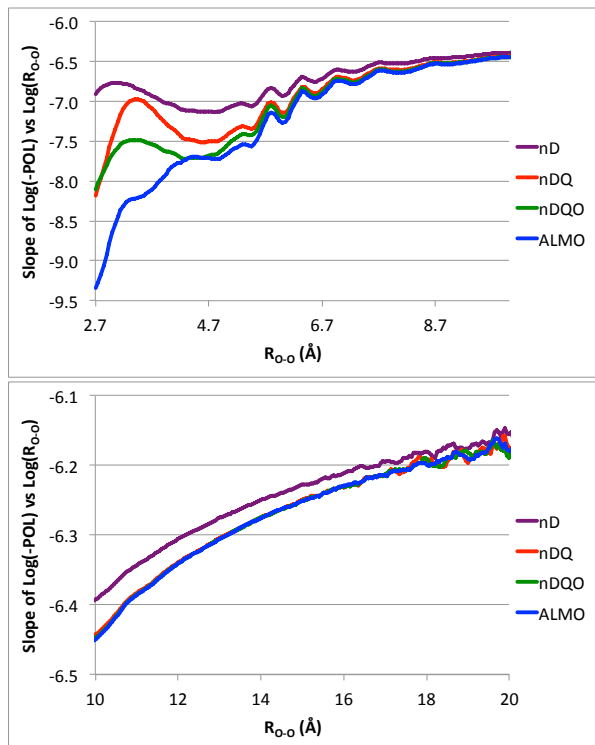

FIG. 3: Polynomial decay of the polarization energy computed using B3LYP/d-aug-cc-pVQZ ALMO and FERF models for the rigid dissociation along the O-O coordinate of the aug-cc-pVQZ/B3LYP optimized water dimer. The slope at point R was computed by linear regression of the log(-POL) vs. log(R_{O-O}) plot for the closest 11 points within 0.25Å of R_{O-O}. The upper panel (a) contains results at shorter O-O separations, demonstrating the different character of the ALMO and FERF models at these distances. The lower panel (b) shows results at longer distances, where the R_{O-O}^{-6} asymptote is approached but not reached before numerical difficulties associated with very small polarization energies arise. Only the least flexible nD model fails to achieve the correct ALMO limiting behavior.

ently from the rest. From this data it would seem that the nD model is potentially inadequate for describing the polarization of molecular systems, and thus nDQ is the simplest FERF model with sufficient accuracy.

We also investigated the convergence of the polarization energy computed by the various non-orthogonal models as a function of basis set cardinal number (i.e. X in aug-cc-pVXZ) for the ammonia dimer (Figure 4a) and methane interacting with a sodium cation (Figure 4b). The ammonia dimer results (Figure 4a) show that the nD model is acceptably converged at aug-cc-pVTZ, nDQ by aug-cc-pVQZ, and nDQO likely by aug-cc-pV5Z based

on the water results above employing more diffuse functions. The angular momentum needs for the polarization of methane in response to a sodium cation (Figure 4b) are by comparison less severe with nD, nDQ, and nDQO all converged by aug-cc-pVQZ.

We analyzed the distance dependence of the polarization models for the qualitatively different CH_4-Na^+ interaction (Figure 5) in the aug-cc-pVQZ basis, which was shown to be sufficient to converge all considered FERF models at equilibrium. The polarization energies computed at compressed distances are not dramatically different for this system, likely
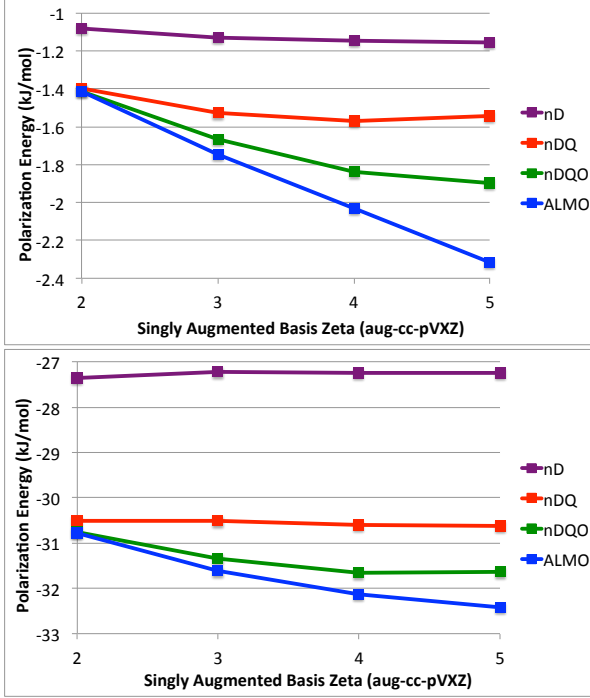
13

FIG. 4: Basis set convergence of B3LYP/aug-cc-pVXZ polarization energies with respect to cardinal number, X, for the ammonia dimer (upper panel, (a)), and the methane-Na^+ complex (lower panel, (b)), both at their B3LYP/aug-cc-pVQZ optimized geometries. Due to the lack of an aug-cc-pV5Z basis set for sodium, the aug-cc-pVQZ basis was used for Na^+ only in the aug-cc-pV5Z calculations.
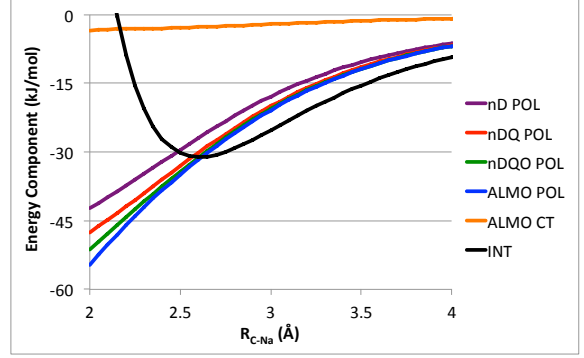

FIG. 5: B3LYP/aug-cc-pVQZ polarization energies by ALMO and FERF models along with total interaction energy (INT) and ALMO charge transfer (CT) contributions for the rigid dissociation of methane-Na^+ along the C-Na coordinate, where the methane fragment is aug-cc-pVQZ/B3LYP optimized.
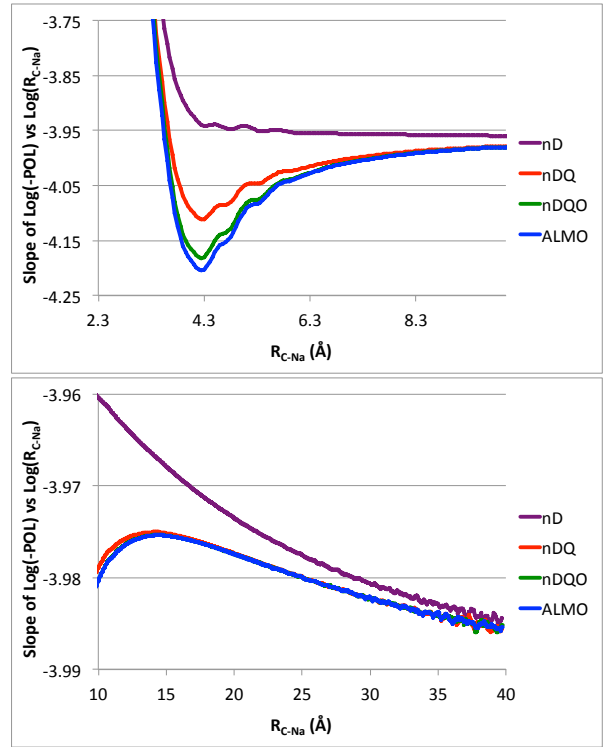

FIG. 6: Polynomial decay of the B3LYP/aug-cc-pVQZ polarization energy computed using ALMO and FERF models for rigid dissociation of methane-Na^+ along the C-Na coordinate, as in Figure 5, with slopes computed as in Figure 3. The upper panel (a) shows polynomial decay of polarization terms for shorter C-Na separations, while the lower panel (b) contains longer range data. In both cases there is a clear difference between the nD model and all others.

because there is little legitimate charge transfer that unduly flexible polarization subspaces could attempt to describe. Figure 6 shows the exponent computed for the polynomial decay of the various polarization models throughout the C-Na coordinate. The nD model distinguishes itself from the others both in the short-range (Figure 6a) and in the long-range (Figure 6b) which asymptotes to R^{-4}, a monopole induced-dipole interaction. All models closely approach R^{-4} decay before polarization energies become too small to compute reliably. As for the water dimer, the nD model behaves qualitatively differently from the others, while both nDQ and nDQO closely track the ALMO results, which should be the correct result at these large separations. Thus, nDQ is again the simplest model with sufficient flexibility to describe the long-range polarization.

We emphasize that, unlike the original ALMO scheme, the new FERF models do have a basis set limit, and it is moreover achievable. Higher order field response models partition more of the sin-

14

gle particle space into fragment-ascribable subspaces with the unwanted consequences of (i) larger basis sets to converge these larger subspaces, as well as (ii) expected ALMO-like behavior of high order models. With this in mind, we recommend the nDQ model as the change in qualitative behavior as well as the computed polarization energy when going from nD to nDQ is palpable while the change in going from nDQ to nDQO seems insufficiently large to justify the increased ambiguity in distinguishing inter- and intra-fragment rotations or the increased cost. The aug-cc-pVQZ basis has been shown to be quite adequate for the nDQ model (aug-cc-pVTZ is nearly adequate), and so QZ basis sets will be used for the DQ models in the remainder of this work.

C. Assessment of Orthogonalized FERF Models

With a model based on responses to weak fields and field gradients decided (FERF/nDQ), we now consider the orthogonalized variant of this scheme. Our first test is the water dimer. The polarization energy lowerings as computed by the nDQ, oDQ, and ALMO models as a function of augmentation of the cc-pVQZ basis are shown in Figure 7. Both the nDQ and oDQ methods yield acceptably converged values at the level of single augmentation though more stringently at double augmentation. Moreover, for all levels of augmentation considered, the oDQ polarization energy lowering is fairly close to but never exceeds that computed by the nDQ model. The gap is less than 1kJ/mol, which may then be viewed as the difference in predictions between the orthogonalized and non-orthogonalized models in the moderately overlapping regime. It is encouraging that this difference is small compared to the magnitude of the nDQ polarization interaction (indeed it is smaller than the nD vs nDQ difference discussed in the previous section). Of course there is no difference between the orthogonal and non-orthogonal FERF variants in the non-overlapping regime.

These same methods have been applied to the water-Na^+ system that was used to motivate the weight matrix construction, (Figure 8a), as well as to the much stronger water-Mg^{2+} interaction (Figure 8b). Both systems show good convergence for the FERF models by aug-cc-pVQZ with over 90% of the nDQ polarization energy lowering recovered by the orthogonal variant, yielding a qualitatively consistent interpretation of the interactions as being polarization dominated in both schemes. While larger than the very small values seen in the ALMO scheme (ALMO E_{CT} is -2.2 kJ/mol for water-Na^+ and -6.8
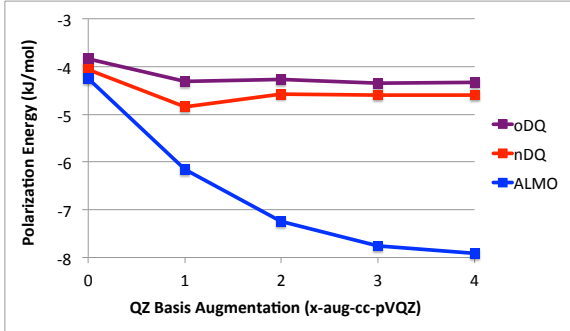

FIG. 7: Convergence with respect to basis augmentation of ALMO and FERF polarization energies computed using B3LYP for the B3LYP/aug-cc-pVQZ optimized water dimer.
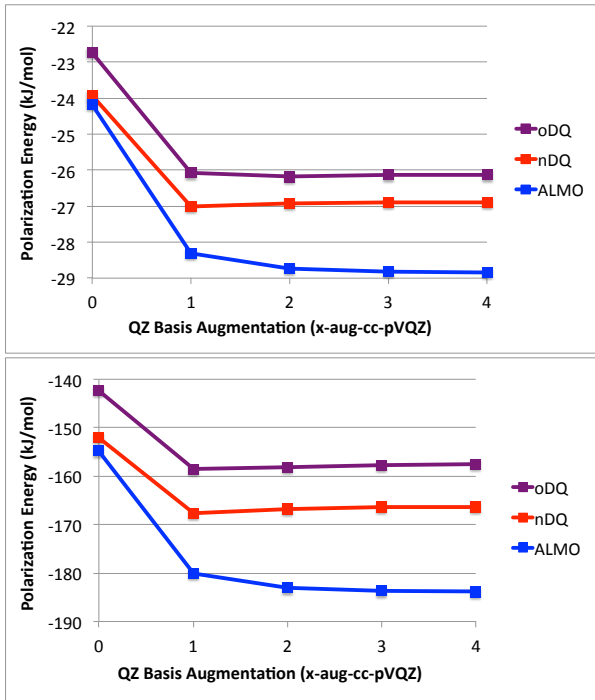

FIG. 8: Convergence with respect to basis augmentation of ALMO and FERF polarization energies computed using B3LYP for water interacting with Na^+ (upper panel, (a)), and Mg^{2+} (lower panel, (b)) at B3LYP/aug-cc-pVQZ optimized geometries.

kJ/mol for water-Mg^{2+} at aug-cc-pVQZ), CT values for the FERF models are still much smaller than the corresponding polarization contributions (even in the oDQ case, which has larger CT contributions than nDQ, E_{CT} is -4.4 kJ/mol for water-Na^+ and -28.3 kJ/mol for water-Mg^{2+} at aug-cc-pVQZ).

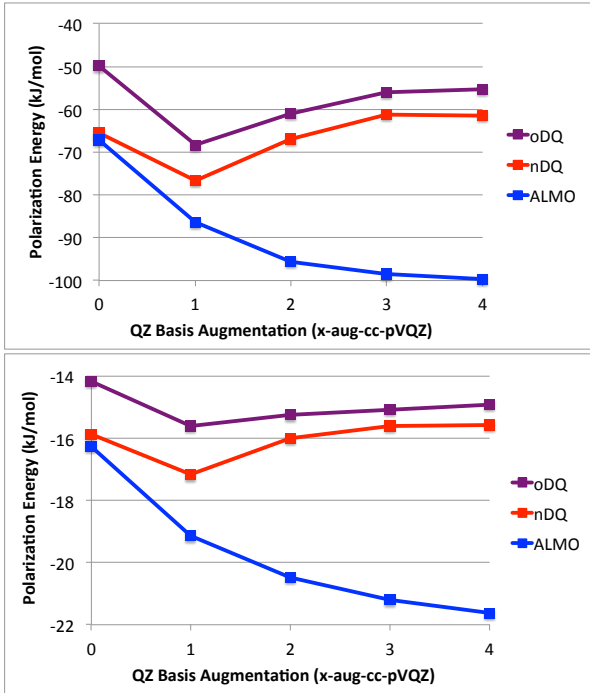We also consider relatively strong (water-F^-, Fig-

FIG. 9: Convergence with respect to basis augmentation of ALMO and FERF polarization energies computed using B3LYP for water interacting with the F^- (upper panel, (a)), and Cl^- (lower panel, (b)) anions, at B3LYP/aug-cc-pVQZ geometries.

ure 9a) and weak (water-Cl^-, Figure 9b) interactions with non-negligible CT contributions. These dimers are interesting tests to explore whether or not the energy difference between the non-orthogonal and orthogonal schemes increases in the presence of significant CT. Both figures, but particularly the fluoride-water results, show the increased difficulty involved in converging DQ responses with respect to basis set augmentation for anionic systems relative to the cationic and neutral systems examined above. This is to be expected as anionic systems require more diffuse functions than the corresponding neutral system to describe the ground state density, and the prerequisites for describing the responses of this density should increase in kind. The more weakly interacting water-Cl^- system is fairly well converged at the level of double augmentation while water-F^- requires a triply augmented basis to converge the orbital response subspace.

One interesting aspect of the results shown in Figure 9 is the pronounced *decrease* in the magnitude of the polarization energy obtained by both the nDQ and oDQ models for the fluoride-water interaction

as the degree of basis set augmentation increases. Does this mean that polarization is over-estimated in the aug-cc-pVQZ basis? We think the answer is no. Rather, we conclude that the basis set limit optimal functions for polarization of the isolated fragment (which is the basis of the FERF models) are not optimal for polarization of the fluoride anion in close contact with the water molecule and vice versa. By this argument (as well as practical imperatives), use of the singly augmented aug-cc-pVQZ basis remains a reasonable choice even for anions, in preference to multiply augmented basis sets.

The fraction of nDQ polarization energy recovered by the oDQ scheme is considerable in both cases though less impressive in the case of water-F^- when compared to the even more strongly interacting water-Mg^{2+} system investigated above. This is likely a consequence of the increased difficulty in meaningfully orthogonalizing the more diffuse functions necessary to describe the anionic system. Furthermore, despite the large CT character of these interactions and the exaggerated problem of tails when orthogonalizing diffuse functions, the oDQ polarization energy does not exceed that of the nDQ model throughout the basis augmentation series.

The last system that we examine in this section is the methyl radical interacting with sodium cation (Figure 10). This system, like its closed shell counterpart, methane-Na^+, discussed above, is expected to have a negligible charge transfer contribution. The occupied and nDQ virtual spans are different for the α and β one-particle subspaces of the methyl radical, and it is the goal of the orthogonalization procedure to maximize the ability of both subspaces to allow the methyl radical density to relax in the presence of the cation. The orthogonalization is quite successful to this end: the gap between nDQ and oDQ is less than 10% of the polarization interaction. In this case, the ALMO model itself is also quite well-behaved, as a consequence of the very small charge-transfer contribution.

The orthogonalization scheme largely accomplishes its aims for the systems investigated here. Should the orthogonal FERF variant, specifically oDQ, be used in practice in preference to the non-orthogonal nDQ model? Though the method is successful, it entails an additional set of arbitrary choices beyond those involved in construction of the naturally non-orthogonal FERFs. The non-orthogonal models have the tremendous advantage of being able to describe the occupied subspace of the isolated fragment, unlike any orthogonal scheme in the overlapping fragment regime. The orthogonal fragment subspaces are also necessarily super-
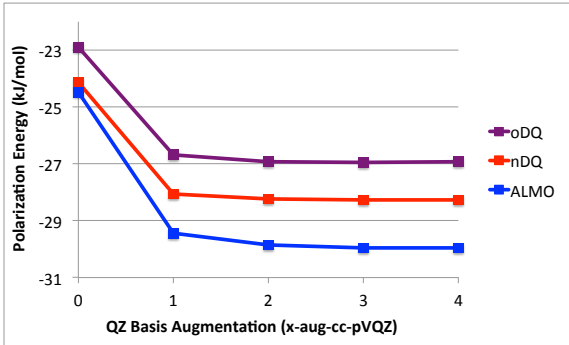
FIG. 10: Convergence with respect to basis augmentation of ALMO and FERF polarization energies computed using B3LYP for methyl radical interacting with Na^+ at the B3LYP/aug-cc-pVQZ optimized geometry (R_{C-Na} = 2.66 Å).

system dependent and are therefore not inherent to a single fragment. Moreover, most variational arguments are sacrificed as the orthogonal subspaces are in general subsets of only the entire one-particle span of the supersystem. However, the orthogonal schemes do have a place in assessing the uncertainty in the construction of fragment subspaces by the non-orthogonal schemes, as they provide a lower bound estimate on the magnitude of the polarization energy lowering.

D. Application of New Polarization Schemes to a Bonded Interaction

The final system that we investigate is the dissociation of ethane into two doublet methyl fragments using the aug-cc-pVQZ basis, which has been shown to be generally sufficient to describe the nDQ and oDQ models in particular. The decomposition of the binding energy using the various polarization models appears in Figure 11a. The considerable difference in results for the different polarization models is not surprising given both the importance of CT interactions and the overall strength of the interaction. The polarization models all give reasonable curves for the polarization energy; however, the choice of model also determines the shape of the CT energy curve (Figure 11b), and not all of these are so reasonable. Notably, the ALMO curve is non-monotonic! The expected CT behavior is to increase with decreasing C-C distance. While still monotonic, the nDQO curve has a similar noticeable change in curvature around the equilibrium separation, and it is not until one decreases SCFMI flexibility to the level of nDQ

subspaces that this feature is largely removed. This finding further illustrates the tendency toward spurious ALMO-like behavior for higher order FERF models (though the nDQO model at aug-cc-pVQZ may not be converged and may be somewhat biased toward ALMO-like behavior).

Figure 11 also contains data for the oD, oDQ, and oDQO polarization models. Unlike most of the previous cases, the oDQ polarization energy deviates appreciably from the nDQ model at compressed bond distances. This difference is larger between oDQO and nDQO and smaller between oD and nD as one might expect given the ranks of their respective polarization subspaces. We note also that the behavior of oDQ is considerably closer to that of oDQO than of oD, suggesting a rather rapid convergence of the orthogonal FERF models with respect to multipole order. The considerable difference between the non-orthogonal and orthogonal polarization models for these short C-C separations indicates a fairly large degree of uncertainty in the numerical values for the polarization and charge transfer contributions provided by each model order in the very strongly overlapping regime.

Whilst Figure 11b reaffirms our preference for lower order FERF models, Figure 12 illustrates the inadequacy of the nD model for the description of polarization in molecular systems as it fails yet again to achieve the ALMO long-range limiting behavior. The expected polarization decay for this system is R_{C-C}^{-6} for a dipole induced-dipole interaction, which is approached but not reached (Figure 12b). The oD, oDQ, and oDQO curves are of course equivalent to the nD, nDQ, and nDQO curves within numerical limitations for appreciable separations where orthogonalization becomes irrelevant, but it is interesting that the oDQ curve (and to a lesser extent oDQO) approximates the limiting R_{C-C}^{-6} decay at noticeably shorter distances than the other methods (Figure 12a). Because of the spurious, ALMO-like behavior of the nDQO model and the deficient long-range polarization in the nD model, we are once again lead to the conclusion that nDQ is the most appropriate non-orthogonal FERF model for polarization. Its orthogonalized counterpart, oDQ, has been shown to be a reasonable indicator for uncertainty, not trivially providing a very similar result to nDQ when interactions are particularly strong.

IV. CONCLUSIONS

In this work, we have presented and applied a method of constructing non-orthogonal and or-
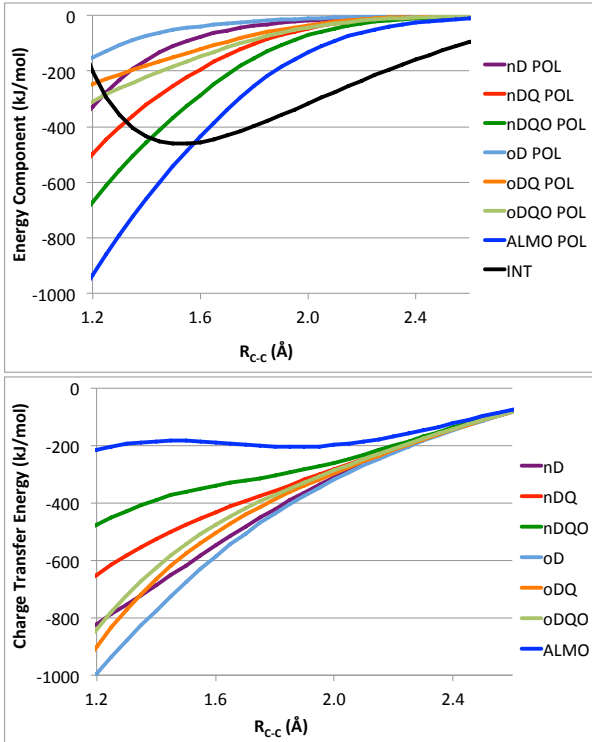
FIG. 11: B3LYP/aug-cc-pVQZ energy components for rigid dissociation of B3LYP/aug-cc-pVTZ optimized ethane along R_{C-C} to form two methyl fragments. The upper panel, (a), shows the polarization energy computed by various models along with the total interaction energy (INT). The difference between the nDQ and oDQ polarization models for compressed geometries indicates intrinsic uncertainty in the numerical values for the polarization and CT contributions provided by these models in the very strongly overlapping regime. The lower panel, (b), shows the CT contributions for ethane dissociation. The curious non-monotonic character of CT in the ALMO model due to a partial description of CT during polarization is removed by the use of the nDQ model.
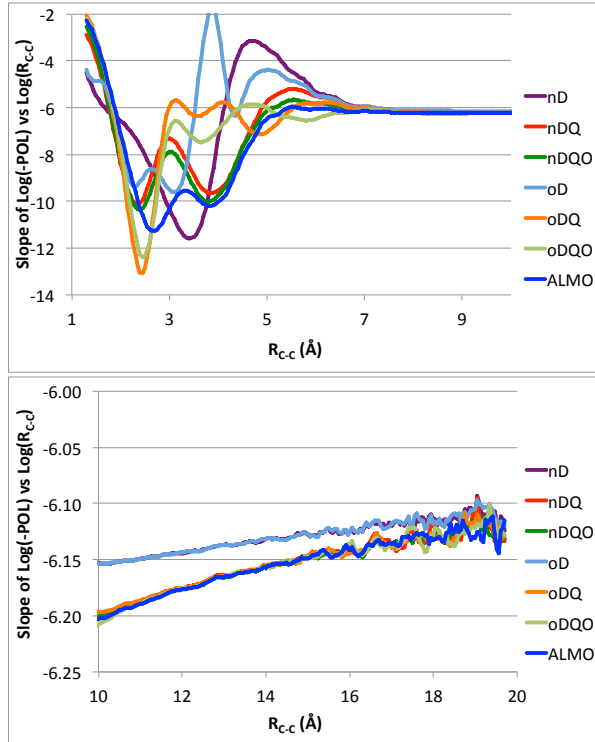
FIG. 12: Polynomial decay of the B3LYP/aug-cc-pVQZ polarization energy using the ALMO and FERF models for dissociation of ethane, using the same level of theory as Figure 11, and the same protocol for tangent evaluation as Figure 3. The upper panel (a), shows the short-range behavior, while the lower panel, (b) shows the long-range behavior. Only the simple nD model fails to achieve the correct ALMO limiting behavior.

thogonal fragment electric-field response functions (FERFs) that exactly describe the polarization of a molecular fragment by an electric field and its spatial derivatives. When applied to a cluster, the FERFs define subspaces of fragment-tagged virtual functions that allow for the definition of a polarization energy (based on solving trivially modified SCFMI equations in the FERF basis) that has the desirable properties listed in the introduction. These properties include basis type independence and a non-trivial basis set limit, which were not features of the AO-subspace SCFMI-based polarization employed by several EDA methods. Our main conclu-

sions are as follows:

1. Test calculations showed that, unlike nD, the FERF nDQ model is capable of describing long-range induced electrostatic interactions in molecular systems. We recommend the smallest adequate FERF model, nDQ, over the nDQO or other higher order models because with the increased flexibility that these higher order models provide, the problems associated with separating polarization and charge transfer in large basis ALMO calculations will be reintroduced. Our investigation of ethane dissociation suggests that this unwanted behavior from undue variational flexibility is already present at the nDQO level. Moreover, it has been shown that reaching the basis set limit for the FERF/nDQ model for polarization is feasible.

2. In practice, the FERF/nDQ model can be satisfactorily employed with a basis set of aug-cc-pVQZ size, and results close to the limit are generally obtained. Even the smaller aug-cc-pVTZ basis appears to give useful results, for systems where aug-cc-pVQZ is too computationally demanding.

3. The orthogonal oDQ scheme was shown for several equilibrium structures to yield polarization energies close to but not exceeding the corresponding nDQ model, demonstrating its utility for approximating a lower bound on the magnitude of the polarization component of interactions. These orthogonalization effects were shown to be relatively small, and therefore there is no *necessity* to use orthogonal schemes, contrary to claims that have periodically been made without numerical support.

4. The only other method for computing polarization energies that meets all of the criteria in the introduction is the CDFT scheme of Wu. We have highlighted a fundamental difference between the degrees of freedom in that scheme and in the SCFMI based schemes.

Only the latter are capable of properly prohibiting charge delocalization during polarization.

5. We intend to incorporate the FERF/nDQ model for describing intra-fragment polarization into a future energy decomposition analysis method, which we hope to report on in due course.

V. ACKNOWLEDGEMENTS

Appendix A: SCFMI Density Matrix First Derivative

Recalling the definition of the density matrix (II.12) and the SCFMI parametrization in terms of orbital rotations (II.18), the first derivative of the density matrix with respect to these degrees of freedom and the necessary partials are:

$$\frac{\partial P_\alpha^{\mu\nu}}{\partial(\Delta_{\alpha,X})_{XpXq}}\bigg|_{\Delta_\alpha=0} = [(\mathbf{I}-\mathbf{P}_\alpha\mathbf{S})\mathbf{G}_\alpha\mathbf{C}_{\alpha,X}\boldsymbol{\sigma}_{\alpha,XX}^{-1}]^{\mu X\bar{r}}[\sum_Z \mathbf{G}_\alpha\mathbf{T}_{\alpha,Z}\boldsymbol{\sigma}_{\alpha,OO}^{-1}]^{\nu Xi}[\delta_r^p\delta_i^q - \delta_i^p\delta_r^q] + \mathrm{Trans}[\mu\nu] \quad \text{(A.1)}$$

$$\frac{\partial(\sigma_{\alpha,OO}^{-1})^{AiBj}}{\partial(\Delta_{\alpha,X})_{XpXq}}\bigg|_{\Delta_\alpha=0} = -\sum_{CD}(\sigma_{\alpha,OO}^{-1})^{AiCk}\left(\frac{\partial(\sigma_\alpha)_{CkDl}}{\partial(\Delta_{\alpha,X})_{XpXq}}\bigg|_{\Delta_\alpha=0}\right)(\sigma_{\alpha,OO}^{-1})^{DlBj} \quad \text{(A.2)}$$

$$\frac{\partial(\sigma_\alpha)_{CkDl}}{\partial(\Delta_{\alpha,X})_{XpXq}}\bigg|_{\Delta_\alpha=0} = [\mathbf{T}_{\alpha,D}^T\boldsymbol{\Gamma}_\alpha\mathbf{C}_{\alpha,C}\boldsymbol{\sigma}_{\alpha,CC}^{-1}]_{Dl\bullet}^{\bullet C\bar{r}}[\delta_r^p\delta_k^q - \delta_r^q\delta_k^p]\delta_C^X + \mathrm{Trans}[CkDl] \quad \text{(A.3)}$$

Appendix B: SCFMI Density Matrix Second Derivative

The second derivative of the density matrix (II.12) with respect to SCFMI rotation parameters (II.18) is:

$$\frac{\partial^2 P_\alpha^{\mu\nu}}{\partial(\Delta_{\alpha,X})_{XpXq}\partial(\Delta_{\alpha,Y})_{YnYo}}\bigg|_{\Delta_\alpha=0} = \text{(B.1)}$$

$$+\frac{1}{2}\delta_Y^X[+\delta_t^p\delta_u^q\delta_v^n\delta_k^o - \delta_t^p\delta_u^q\delta_v^o\delta_k^n - \delta_t^q\delta_u^p\delta_v^n\delta_k^o + \delta_t^q\delta_u^p\delta_v^o\delta_k^n$$

$$+\delta_t^n\delta_u^o\delta_v^p\delta_k^q - \delta_t^n\delta_u^o\delta_v^q\delta_k^p - \delta_t^o\delta_u^n\delta_v^p\delta_k^q + \delta_t^o\delta_u^n\delta_v^q\delta_k^p]$$

$$\times[(\mathbf{I}-\mathbf{P}_\alpha\mathbf{S})\mathbf{G}_\alpha\mathbf{C}_{\alpha,X}\boldsymbol{\sigma}_{\alpha,XX}^{-1}]^{\mu X\bar{t}}(\sigma_{\alpha,XX}^{-1})^{X\bar{u}X\bar{v}}[\sum_Z\mathbf{G}_\alpha\mathbf{T}_{\alpha,Z}\boldsymbol{\sigma}_{\alpha,OO}^{-1}]^{\nu Xk}$$

$$+[\delta_l^p\delta_s^q\delta_k^n\delta_t^o - \delta_l^p\delta_s^q\delta_k^o\delta_t^n - \delta_l^q\delta_s^p\delta_k^n\delta_t^o + \delta_l^q\delta_s^p\delta_k^o\delta_t^n]$$

$$\times\Big[[(\mathbf{I}-\mathbf{P}_\alpha\mathbf{S})\mathbf{G}_\alpha\mathbf{C}_{\alpha,X}\boldsymbol{\sigma}_{\alpha,XX}^{-1}]^{\mu X\bar{s}}(\sigma_{\alpha,OO}^{-1})^{XlYk}[(\mathbf{I}-\mathbf{P}_\alpha\mathbf{S})\mathbf{G}_\alpha\mathbf{C}_{\alpha,Y}\boldsymbol{\sigma}_{\alpha,YY}^{-1}]^{\nu Y\bar{t}}$$

$$-[(\mathbf{I}-\mathbf{P}_\alpha\mathbf{S})\mathbf{G}_\alpha\mathbf{C}_{\alpha,Y}\boldsymbol{\sigma}_{\alpha,YY}^{-1}]^{\mu Y\bar{t}}[\sum_Z\mathbf{G}_\alpha\mathbf{T}_{\alpha,Z}\boldsymbol{\sigma}_{\alpha,OO}^{-1}]^{\nu Xl}[\sum_W\boldsymbol{\sigma}_{\alpha,OO}^{-1}\mathbf{T}_{\alpha,W}^T\boldsymbol{\Gamma}_\alpha\mathbf{C}_{\alpha,X}\boldsymbol{\sigma}_{\alpha,XX}^{-1}]^{YkX\bar{s}}$$

$$-[(\mathbf{I}-\mathbf{P}_\alpha\mathbf{S})\mathbf{G}_\alpha\mathbf{C}_{\alpha,X}\boldsymbol{\sigma}_{\alpha,XX}^{-1}]^{\mu X\bar{s}}[\sum_Z\mathbf{G}_\alpha\mathbf{T}_{\alpha,Z}\boldsymbol{\sigma}_{\alpha,OO}^{-1}]^{\nu Yk}[\sum_W\boldsymbol{\sigma}_{\alpha,OO}^{-1}\mathbf{T}_{\alpha,W}^T\boldsymbol{\Gamma}_\alpha\mathbf{C}_{\alpha,Y}\boldsymbol{\sigma}_{\alpha,YY}^{-1}]^{XlY\bar{t}}$$

$$-[\sum_Z\mathbf{G}_\alpha\mathbf{T}_{\alpha,Z}\boldsymbol{\alpha}_{\alpha,OO}^{-1}]^{\mu Xl}[\sum_W\mathbf{G}_\alpha\mathbf{T}_{\alpha,W}\boldsymbol{\alpha}_{\alpha,OO}^{-1}]^{\nu Yk}[\boldsymbol{\sigma}_{\alpha,YY}^{-1}\mathbf{C}_{\alpha,Y}^T\mathbf{G}_\alpha^T(\mathbf{S}-\mathbf{S}\mathbf{P}_\alpha\mathbf{S})\mathbf{G}_\alpha\mathbf{C}_{\alpha,X}\boldsymbol{\sigma}_{\alpha,XX}^{-1}]^{Y\bar{t}X\bar{s}}\Big]$$

$$+\text{Trans}[\mu\nu]$$

The necessary partials in addition to (A.2) and (A.3) are:

$$\left.\frac{\partial^2(\sigma_{\alpha,OO}^{-1})^{AiBj}}{\partial(\Delta_{\alpha,X})_{XpXq}\partial(\Delta_{\alpha,Y})_{YnYo}}\right|_{\Delta_\alpha=0} = \tag{B.2}$$

$$-\sum_{CD}(\sigma_{\alpha,OO}^{-1})^{AiCk}\left(\left.\frac{\partial^2(\sigma_\alpha)_{CkDl}}{\partial(\Delta_{\alpha,X})_{XpXq}\partial(\Delta_{\alpha,Y})_{YnYo}}\right|_{\Delta_\alpha=0}\right)(\sigma_{\alpha,OO}^{-1})^{DlBj}$$

$$+\sum_{CDEF}(\sigma_{\alpha,OO}^{-1})^{AiCk}\left(\left.\frac{\partial(\sigma_\alpha)_{CkDl}}{\partial(\Delta_{\alpha,X})_{XpXq}}\right|_{\Delta_\alpha=0}\right)(\sigma_{\alpha,OO}^{-1})^{DlEe}\left(\left.\frac{\partial(\sigma_\alpha)_{EeFf}}{\partial(\Delta_{\alpha,Y})_{YnYo}}\right|_{\Delta_\alpha=0}\right)(\sigma_{\alpha,OO}^{-1})^{FfBj}$$

$$+\sum_{CDEF}(\sigma_{\alpha,OO}^{-1})^{AiEe}\left(\left.\frac{\partial(\sigma_\alpha)_{EeFf}}{\partial(\Delta_{\alpha,Y})_{YnYo}}\right|_{\Delta_\alpha=0}\right)(\sigma_{\alpha,OO}^{-1})^{FfCk}\left(\left.\frac{\partial(\sigma_\alpha)_{CkDl}}{\partial(\Delta_{\alpha,X})_{XpXq}}\right|_{\Delta_\alpha=0}\right)(\sigma_{\alpha,OO}^{-1})^{DlBj}$$

$$\left.\frac{\partial^2(\sigma_\alpha)_{CkDl}}{\partial(\Delta_{\alpha,X})_{XpXq}\partial(\Delta_{\alpha,Y})_{YnYo}}\right|_{\Delta_\alpha=0} = \tag{B.3}$$

$$+\frac{1}{2}\delta_C^X\delta_C^Y[\mathbf{T}_{\alpha,D}^T\boldsymbol{\Gamma}_\alpha\mathbf{C}_{\alpha,C}\boldsymbol{\sigma}_{\alpha,CC}^{-1}]_{Dl\bullet}^{\bullet C\bar{t}}(\sigma_{\alpha,CC}^{-1})^{C\bar{u}C\bar{v}}$$

$$\times[+\delta_t^p\delta_u^q\delta_v^n\delta_k^o - \delta_t^p\delta_u^q\delta_k^n\delta_v^o - \delta_u^p\delta_t^q\delta_v^n\delta_k^o + \delta_u^p\delta_t^q\delta_k^n\delta_v^o$$

$$+\delta_t^n\delta_u^o\delta_v^p\delta_k^q - \delta_t^n\delta_u^o\delta_k^p\delta_v^q - \delta_u^n\delta_t^o\delta_v^p\delta_k^q + \delta_u^n\delta_t^o\delta_k^p\delta_v^q]$$

$$+\delta_C^X\delta_D^Y[\boldsymbol{\sigma}_{\alpha,XX}^{-1}\boldsymbol{\sigma}_\alpha\boldsymbol{\sigma}_{\alpha,YY}^{-1}]^{X\bar{t}Y\overline{w}}$$

$$\times[\delta_t^p\delta_k^q\delta_w^n\delta_l^o - \delta_k^p\delta_t^q\delta_w^n\delta_l^o - \delta_t^p\delta_k^q\delta_l^n\delta_w^o + \delta_k^p\delta_t^q\delta_l^n\delta_w^o]$$

$$+\text{Trans}[CkDl]$$

Appendix C: SCFMI Energy Orbital Hessian

The second derivative of the electronic energy with respect to SCFMI orbital rotations is:

$$\left.\frac{\partial^2 E}{\partial(\Delta_{\alpha,X})_{XpXq}\partial(\Delta_{\beta,Y})_{YnYo}}\right|_{\Delta_\alpha=0} \tag{C.1}$$

$$= \frac{\partial E}{\partial P_\alpha^{\mu\nu}}\left.\frac{\partial^2 P_\alpha^{\mu\nu}}{\partial(\Delta_{\alpha,X})_{XpXq}\partial(\Delta_{\beta,Y})_{YnYo}}\right|_{\Delta_\alpha=0}$$

$$+\left.\frac{\partial(P_\alpha)^{\mu\nu}}{\partial(\Delta_{\alpha,X})_{XpXq}}\right|_{\Delta_\alpha=0}\frac{\partial^2 E}{\partial P_\alpha^{\mu\nu}\partial P_\beta^{\lambda\sigma}}\left.\frac{\partial(P_\beta)^{\lambda\sigma}}{\partial(\Delta_{\beta,Y})_{YnYo}}\right|_{\Delta_\alpha=0}$$

This expression can be simplified using (II.15), (D.6), (A.1), and (B.1) to yield the Hessian without the assumption of intra-subspace orthogonality:

$$\frac{\partial^2 E}{\partial(\Delta_{\alpha,X})_{XpXq}\partial(\Delta_{\beta,Y})_{YnYo}}\Bigg|_{\Delta_\alpha=0} = \quad \text{(C.2)}$$

$$+\delta_Y^X\delta_\beta^\alpha[+\delta_t^p\delta_u^q\delta_v^n\delta_k^o - \delta_t^p\delta_u^q\delta_v^o\delta_k^n - \delta_t^q\delta_u^p\delta_v^n\delta_k^o + \delta_t^q\delta_u^p\delta_v^o\delta_k^n$$

$$+\delta_t^n\delta_u^o\delta_v^p\delta_k^q - \delta_t^n\delta_u^o\delta_v^q\delta_k^p - \delta_t^o\delta_u^n\delta_v^p\delta_k^q + \delta_t^o\delta_u^n\delta_v^q\delta_k^p]$$

$$\times[\sum_Z \boldsymbol{\sigma}_{\alpha,OO}^{-1}\mathbf{T}_{\alpha,Z}^T\mathbf{G}_\alpha^T\mathbf{F}_\alpha(\mathbf{I}-\mathbf{P}_\alpha\mathbf{S})\mathbf{G}_\alpha\mathbf{C}_{\alpha,X}\boldsymbol{\sigma}_{\alpha,XX}^{-1}]^{XkX\bar{t}}\sigma_\alpha^{X\bar{u}X\bar{v}}$$

$$+2\delta_\beta^\alpha[\delta_l^p\delta_s^q\delta_k^n\delta_t^o - \delta_l^p\delta_s^q\delta_k^o\delta_t^n - \delta_l^q\delta_s^p\delta_k^n\delta_t^o + \delta_l^q\delta_s^p\delta_k^o\delta_t^n]$$

$$\times\left[(\sigma_{\alpha,OO}^{-1})^{XlYk}[\boldsymbol{\sigma}_{\alpha,XX}^{-1}\mathbf{C}_{\alpha,X}^T\mathbf{G}_\alpha^T(\mathbf{I}-\mathbf{SP}_\alpha)\mathbf{F}_\alpha(\mathbf{I}-\mathbf{P}_\alpha\mathbf{S})\mathbf{G}_\alpha\mathbf{C}_{\alpha,Y}\boldsymbol{\sigma}_{\alpha,YY}^{-1}]^{X\bar{s}Y\bar{t}}\right.$$

$$-[\sum_Z \boldsymbol{\sigma}_{\alpha,OO}^{-1}\mathbf{T}_{\alpha,Z}^T\mathbf{G}_\alpha^T\mathbf{F}_\alpha(\mathbf{I}-\mathbf{P}_\alpha\mathbf{S})\mathbf{G}_\alpha\mathbf{C}_{\alpha,Y}\boldsymbol{\sigma}_{\alpha,YY}^{-1}]^{XlY\bar{t}}[\sum_W \boldsymbol{\sigma}_{\alpha,OO}^{-1}\mathbf{T}_{\alpha,W}^T\boldsymbol{\Gamma}_\alpha\mathbf{C}_{\alpha,X}\boldsymbol{\sigma}_{\alpha,XX}^{-1}]^{YkX\bar{s}}$$

$$-[\sum_Z \boldsymbol{\sigma}_{\alpha,OO}^{-1}\mathbf{T}_{\alpha,Z}^T\mathbf{G}_\alpha^T\mathbf{F}_\alpha(\mathbf{I}-\mathbf{P}_\alpha\mathbf{S})\mathbf{G}_\alpha\mathbf{C}_{\alpha,X}\boldsymbol{\sigma}_{\alpha,XX}^{-1}]^{YkX\bar{s}}[\sum_W \boldsymbol{\sigma}_{\alpha,OO}^{-1}\mathbf{T}_{\alpha,W}^T\boldsymbol{\Gamma}_\alpha\mathbf{C}_{\alpha,Y}\boldsymbol{\sigma}_{\alpha,YY}^{-1}]^{XlY\bar{t}}$$

$$\left.-[\sum_{WZ} \boldsymbol{\sigma}_{\alpha,OO}^{-1}\mathbf{T}_{\alpha,Z}^T\mathbf{G}_\alpha^T\mathbf{F}_\alpha\mathbf{G}_\alpha\mathbf{T}_{\alpha,W}\boldsymbol{\sigma}_{\alpha,OO}^{-1}]^{YkXl}[\boldsymbol{\sigma}_{\alpha,YY}^{-1}\mathbf{C}_{\alpha,Y}^T\mathbf{G}_\alpha^T(\mathbf{S}-\mathbf{SP}_\alpha\mathbf{S})\mathbf{G}_\alpha\mathbf{C}_{\alpha,X}\boldsymbol{\sigma}_{\alpha,XX}^{-1}]^{Y\bar{t}X\bar{s}}\right]$$

$$+4[\delta_r^p\delta_i^q - \delta_i^p\delta_r^q][\delta_s^n\delta_j^o - \delta_j^n\delta_s^o](\Pi_{\alpha\beta})_{\mu\nu\lambda\sigma}$$

$$\times[(\mathbf{I}-\mathbf{P}_\alpha\mathbf{S})\,\mathbf{G}_\alpha\mathbf{C}_{\alpha,X}(\boldsymbol{\sigma}_{\alpha,XX})^{-1}]^{\mu X\bar{r}}[\sum_Z \mathbf{G}_\alpha\mathbf{T}_{\alpha,Z}(\boldsymbol{\sigma}_{\alpha,OO})^{-1}]^{\nu Xi}$$

$$\times[(\mathbf{I}-\mathbf{P}_\beta\mathbf{S})\,\mathbf{G}_\beta\mathbf{C}_{\beta,Y}(\boldsymbol{\sigma}_{\beta,YY})^{-1}]^{\lambda Y\bar{s}}[\sum_W \mathbf{G}_\beta\mathbf{T}_{\beta,W}(\boldsymbol{\sigma}_{\beta,OO})^{-1}]^{\sigma Yj}$$

Appendix D: SCFMI Energy Preconditioning Strategy

The SCFMI orbital Hessian in the case of intra-subspace orthogonality is as follows (where we are reverting to considering the spin cases explicitly, as indicated by the spin labels):

$$\frac{\partial^2 E}{\partial(\Delta_{\alpha,A})_{AiAa}\partial(\Delta_{\beta,B})_{BjBb}}\Bigg|_{\{\Delta\}=0} = \quad \text{(D.1)}$$

$$\delta_\beta^\alpha 2\left[(\boldsymbol{\sigma}_{\alpha,OO})^{-1}\right]^{AiBj}\left[\mathbf{V}_{\alpha,A}^T\mathbf{G}_\alpha^T(\mathbf{I}-\mathbf{SP}_\alpha)\,\mathbf{F}_\alpha(\mathbf{I}-\mathbf{P}_\alpha\mathbf{S})\,\mathbf{G}_\alpha\mathbf{V}_{\alpha,B}\right]_{AaBb} \quad \text{(D.2)}$$

$$-\delta_\beta^\alpha 2\left[\sum_Z(\boldsymbol{\sigma}_{\alpha,OO})^{-1}\mathbf{T}_{\alpha,Z}^T\boldsymbol{\Gamma}_\alpha\mathbf{V}_{\alpha,B}\right]_{\bullet Bb}^{Ai\bullet}\left[\sum_Y(\boldsymbol{\sigma}_{\alpha,OO})^{-1}\mathbf{T}_{\alpha,Y}^T\mathbf{G}_\alpha^T\mathbf{F}_\alpha(\mathbf{I}-\mathbf{P}_\alpha\mathbf{S})\,\mathbf{G}_\alpha\mathbf{V}_{\alpha,A}\right]_{\bullet Aa}^{Bj\bullet} \quad \text{(D.3)}$$

$$-\delta_\beta^\alpha 2\left[\sum_Z(\boldsymbol{\sigma}_{\alpha,OO})^{-1}\mathbf{T}_{\alpha,Z}^T\boldsymbol{\Gamma}_\alpha\mathbf{V}_{\alpha,A}\right]_{\bullet Aa}^{Bj\bullet}\left[\sum_Y(\boldsymbol{\sigma}_{\alpha,OO})^{-1}\mathbf{T}_{\alpha,Y}^T\mathbf{G}_\alpha^T\mathbf{F}_\alpha(\mathbf{I}-\mathbf{P}_\alpha\mathbf{S})\,\mathbf{G}_\alpha\mathbf{V}_{\alpha,B}\right]_{\bullet Bb}^{Ai\bullet} \quad \text{(D.4)}$$

$$-\delta_\beta^\alpha 2\left[\mathbf{V}_{\alpha,A}^T\mathbf{G}_\alpha^T(\mathbf{S}-\mathbf{SP}_\alpha\mathbf{S})\,\mathbf{G}_\alpha\mathbf{V}_{\alpha,B}\right]_{AaBb}\left[\sum_{YZ}(\boldsymbol{\sigma}_{\alpha,OO})^{-1}\mathbf{T}_{\alpha,Z}^T\mathbf{G}_\alpha^T\mathbf{F}_\alpha\mathbf{G}_\alpha\mathbf{T}_{\alpha,Y}(\boldsymbol{\sigma}_{\alpha,OO})^{-1}\right]^{AiBj} \quad \text{(D.5)}$$

$$+4[(\mathbf{I}-\mathbf{P}_\alpha\mathbf{S})\,\mathbf{G}_\alpha\mathbf{V}_{\alpha,A}]_{\bullet Aa}^{\mu\bullet}\left[\sum_Z(\boldsymbol{\sigma}_{\alpha,OO})^{-1}\mathbf{T}_{\alpha,Z}^T\mathbf{G}_\alpha^T\right]^{Ai\nu}(\Pi_{\alpha\beta})_{\mu\nu\lambda\sigma}$$

$$\times[(\mathbf{I}-\mathbf{P}_\beta\mathbf{S})\,\mathbf{G}_\beta\mathbf{V}_{\beta,B}]_{\bullet Bb}^{\lambda\bullet}\left[\sum_Y(\boldsymbol{\sigma}_{\beta,OO})^{-1}\mathbf{T}_{\beta,Y}^T\mathbf{G}_\beta^T\right]^{Bj\sigma}$$

where:

$$(\Pi_{\alpha\beta})_{\mu\nu\lambda\sigma} \equiv \frac{\partial^2 E}{\partial P_\alpha^{\mu\nu} \partial P_\beta^{\lambda\sigma}} \qquad (D.6)$$

The tensor $\mathbf{\Pi}$ involves the two electron integrals and second derivatives of the exchange correlation energy in the case of DFT. Apparent inconsistences in the covariant-contravariant notation are a consequence of the omission of metrics equivalent to the identity. The contraction of the SCFMI Hessian with a trial vector for the solution of the Newton step by conjugate gradient or MINRES is straightforward.

We have considered two levels of preconditioning for the solution of this linear equation, and we use these same approximate inverse Hessians to augment the quasi-Newton algorithm. The less expensive of the two preconditioners considers terms from $E^P \cdot P^{\Delta\Delta}$, lines (D.2) through (D.5), assuming weakly overlapping fragments such that overlap-like terms can be approximated by kronecker deltas:

$$(B_\alpha)^{(A\bar{i}A\bar{a})\bullet}_{\bullet\ R} = \qquad (D.7)$$
$$(H_{\alpha\alpha}^{approx.})^{(A\bar{i}A\bar{a})(A\bar{j}A\bar{b})}(X_\alpha)_{(AjAb)R}$$

$$(H_{\alpha\alpha}^{approx.})^{(A\bar{i}A\bar{a})(A\bar{j}A\bar{b})} = \qquad (D.8)$$
$$\left[\mathbf{V}_{\alpha,A}^T \mathbf{G}_\alpha^T (\mathbf{I} - \mathbf{SP}_\alpha) \mathbf{F}_\alpha (\mathbf{I} - \mathbf{P}_\alpha \mathbf{S}) \mathbf{G}_\alpha \mathbf{V}_{\alpha B}\right]_{AaAb}$$
$$\times\, 2\delta_{AiAj} - 2\delta_{AaAb}$$
$$\times \left[\sum_{YZ}(\boldsymbol{\sigma}_{\alpha,OO})^{-1}\mathbf{T}_{\alpha,Z}^T \mathbf{G}_\alpha^T \mathbf{F}_\alpha \mathbf{G}_\alpha \mathbf{T}_{\alpha,Y}(\boldsymbol{\sigma}_{\alpha,OO})^{-1}\right]^{AiAj}$$

$\mathbf{B}$ is the matrix of column vectors (R) with potentially alpha and beta portions to be preconditioned (our approximate Hessian is spin-block-diagonal), and $\mathbf{X}$ are the preconditioned vectors. The linear equation defined by (D.7) and (D.8) can easily be solved by the application of pseudocanonical-like intra-subspace occupied-occupied and virtual-virtual rotations, which bring the approximate Hessian (D.8) into diagonal form.

A more expensive but still linear scaling preconditioner which does not involve the contraction of trial vectors with two-electron integrals or XC matrix derivatives considers all subspace-diagonal blocks of terms from $E^P \cdot P^{\Delta\Delta}$, (D.2) through (D.5), which are again spin-diagonal:

$$(H_{\alpha\alpha}^{approx.})^{(A\bar{i}A\bar{a})(A\bar{j}A\bar{b})} = \qquad (D.9)$$
$$2\left((\boldsymbol{\sigma}_{\alpha,OO})^{-1}\right)^{AiAj}\left[\mathbf{V}_{\alpha,A}^T \mathbf{G}_\alpha^T (\mathbf{I} - \mathbf{SP}_\alpha) \mathbf{F}_\alpha (\mathbf{I} - \mathbf{P}_\alpha \mathbf{S}) \mathbf{G}_\alpha \mathbf{V}_{\alpha A}\right]_{AaAb}$$
$$- 2\left[\sum_Z (\boldsymbol{\sigma}_{\alpha,OO})^{-1}\mathbf{T}_{\alpha,Z}^T \boldsymbol{\Gamma}_\alpha \mathbf{V}_{\alpha,A}\right]^{Ai\,\bullet}_{\bullet\,Ab}\left[\sum_Y (\boldsymbol{\sigma}_{\alpha,OO})^{-1}\mathbf{T}_{\alpha,Y}^T \mathbf{G}_\alpha^T \mathbf{F}_\alpha (\mathbf{I} - \mathbf{P}_\alpha \mathbf{S}) \mathbf{G}_\alpha \mathbf{V}_{\alpha,A}\right]^{Aj\,\bullet}_{\bullet\,Aa}$$
$$- 2\left[\sum_Z (\boldsymbol{\sigma}_{\alpha,OO})^{-1}\mathbf{T}_{\alpha,Z}^T \boldsymbol{\Gamma}_\alpha \mathbf{V}_{\alpha,A}\right]^{Aj\,\bullet}_{\bullet\,Aa}\left[\sum_Y (\boldsymbol{\sigma}_{\alpha,OO})^{-1}\mathbf{T}_{\alpha,Y}^T \mathbf{G}_\alpha^T \mathbf{F}_\alpha (\mathbf{I} - \mathbf{P}_\alpha \mathbf{S}) \mathbf{G}_\alpha \mathbf{V}_{\alpha,A}\right]^{Ai\,\bullet}_{\bullet\,Ab}$$
$$- 2\left[\mathbf{V}_{\alpha,A}^T \mathbf{G}_\alpha^T (\mathbf{S} - \mathbf{SP}_\alpha \mathbf{S}) \mathbf{G}_\alpha \mathbf{V}_{\alpha,A}\right]_{AaAb}\left[\sum_{YZ}(\boldsymbol{\sigma}_{\alpha,OO})^{-1}\mathbf{T}_{\alpha,Z}^T \mathbf{G}_\alpha^T \mathbf{F}_\alpha \mathbf{G}_\alpha \mathbf{T}_{\alpha,Y}(\boldsymbol{\sigma}_{\alpha,OO})^{-1}\right]^{AiAj}$$

The solution of the linear system defined by (D.7) and (D.9) can be computed separately for each subspace by a linear solver such as conjugate gradient using a more approximate and less expensive preconditioner such as (D.8). One could continue nesting preconditioners in this way to precondition with all of $E^P \cdot P^{\Delta\Delta}$, (D.2) through (D.5), but the inclusion of inter-subspace blocks makes the matrix application to a trial vector quadratic in subspaces. This is in general an undesirable cost increase for quasi-Newton methods; however, it has been a helpful strategy in the context of preconditioning the conjugate gradient iterations for the solution of Newton steps where the expensive operation is multiplication by the entire Hessian (D.1), which requires the additional, more expensive contractions with Π. We note that other authors[79,80] have previously employed full BFGS initialized with an approximate Hessian to solve the SCFMI problem. The approach taken in this work uses a newly calculated and thus

more relevant approximate Hessian as a preconditioner at each L-BFGS iteration and requires only the application of this matrix to a vector, never its storage.

Appendix E: SCFMI Population Derivatives

The first derivative of the population of domain A with respect to SCFMI rotation parameters by (II.26) and (A.1) is:

$$\frac{\partial \mathrm{Pop}_{\alpha,A}}{\partial(\Delta_{\alpha,X})_{XpXq}}\bigg|_{\Delta_\alpha=0} = \frac{\partial \mathrm{Pop}_{\alpha,A}}{\partial P_\alpha^{\mu\nu}}\frac{\partial P_\alpha^{\mu\nu}}{\partial(\Delta_{\alpha,X})_{XpXq}}\bigg|_{\Delta_\alpha=0} \quad (E.1)$$

$$= [\delta_r^p\delta_i^q - \delta_i^p\delta_r^q][\sum_Z (\boldsymbol{\sigma}_{\alpha,OO})^{-1}\mathbf{T}_{\alpha,Z}^T\mathbf{G}_\alpha^T\mathbf{S}(\mathbf{P}_{\alpha,A}+\mathbf{P}_{\alpha,A}^T)$$

$$\times \mathbf{S}(\mathbf{I}-\mathbf{P}_\alpha\mathbf{S})\mathbf{G}_\alpha\mathbf{C}_{\alpha,X}(\boldsymbol{\sigma}_{\alpha,XX})^{-1}]^{Xi X\bar{r}}$$

The second derivative of the population of domain A with respect to SCFMI rotation parameters by (II.26) and (B.1) is:

$$\frac{\partial^2 \mathrm{Pop}_{\alpha,A}}{\partial(\Delta_{\alpha,X})_{XpXq}\partial(\Delta_{\alpha,Y})_{YnYo}}\bigg|_{\Delta_\alpha=0} \quad (E.2)$$

$$+\delta_Y^X\frac{1}{2}[+\delta_t^p\delta_u^q\delta_v^n\delta_k^o - \delta_t^p\delta_u^q\delta_v^o\delta_k^n - \delta_t^q\delta_u^p\delta_v^n\delta_k^o + \delta_t^q\delta_u^p\delta_v^o\delta_k^n$$

$$+\delta_t^n\delta_u^o\delta_v^p\delta_k^q - \delta_t^n\delta_u^o\delta_v^q\delta_k^p - \delta_t^o\delta_u^n\delta_v^p\delta_k^q + \delta_t^o\delta_u^n\delta_v^q\delta_k^p]$$

$$\times[\sum_Z \boldsymbol{\sigma}_{\alpha,OO}^{-1}\mathbf{T}_{\alpha,Z}^T\mathbf{G}_\alpha^T\mathbf{S}(\mathbf{P}_{\alpha,A}+\mathbf{P}_{\alpha,A}^T)\mathbf{S}(\mathbf{I}-\mathbf{P}_\alpha\mathbf{S})\mathbf{G}_\alpha\mathbf{C}_{\alpha,X}\boldsymbol{\sigma}_{\alpha,XX}^{-1}]^{XkX\bar{t}}\sigma_\alpha^{X\bar{u}X\bar{v}}$$

$$+[\delta_l^p\delta_s^q\delta_k^n\delta_t^o - \delta_l^p\delta_s^q\delta_k^o\delta_t^n - \delta_l^q\delta_s^p\delta_k^n\delta_t^o + \delta_l^q\delta_s^p\delta_k^o\delta_t^n]$$

$$\times\bigg[(\sigma_{\alpha,OO}^{-1})^{XlYk}[\boldsymbol{\sigma}_{\alpha,XX}^{-1}\mathbf{C}_{\alpha,X}^T\mathbf{G}_\alpha^T(\mathbf{I}-\mathbf{SP}_\alpha)\mathbf{S}(\mathbf{P}_{\alpha,A}+\mathbf{P}_{\alpha,A}^T)\mathbf{S}(\mathbf{I}-\mathbf{P}_\alpha\mathbf{S})\mathbf{G}_\alpha\mathbf{C}_{\alpha,Y}\boldsymbol{\sigma}_{\alpha,YY}^{-1}]^{X\bar{s}Y\bar{t}}$$

$$-[\sum_Z \boldsymbol{\sigma}_{\alpha,OO}^{-1}\mathbf{T}_{\alpha,Z}^T\mathbf{G}_\alpha^T\mathbf{S}(\mathbf{P}_{\alpha,A}+\mathbf{P}_{\alpha,A}^T)\mathbf{S}(\mathbf{I}-\mathbf{P}_\alpha\mathbf{S})\mathbf{G}_\alpha\mathbf{C}_{\alpha,Y}\boldsymbol{\sigma}_{\alpha,YY}^{-1}]^{XlY\bar{t}}[\sum_W \boldsymbol{\sigma}_{\alpha,OO}^{-1}\mathbf{T}_{\alpha,W}^T\boldsymbol{\Gamma}_\alpha\mathbf{C}_{\alpha,X}\boldsymbol{\sigma}_{\alpha,XX}^{-1}]^{YkX\bar{s}}$$

$$-[\sum_Z \boldsymbol{\sigma}_{\alpha,OO}^{-1}\mathbf{T}_{\alpha,Z}^T\mathbf{G}_\alpha^T\mathbf{S}(\mathbf{P}_{\alpha,A}+\mathbf{P}_{\alpha,A}^T)\mathbf{S}(\mathbf{I}-\mathbf{P}_\alpha\mathbf{S})\mathbf{G}_\alpha\mathbf{C}_{\alpha,X}\boldsymbol{\sigma}_{\alpha,XX}^{-1}]^{YkX\bar{s}}[\sum_W \boldsymbol{\sigma}_{\alpha,OO}^{-1}\mathbf{T}_{\alpha,W}^T\boldsymbol{\Gamma}_\alpha\mathbf{C}_{\alpha,Y}\boldsymbol{\sigma}_{\alpha,YY}^{-1}]^{XlY\bar{t}}$$

$$-[\sum_{ZW} \boldsymbol{\sigma}_{\alpha,OO}^{-1}\mathbf{T}_{\alpha,Z}^T\mathbf{G}_\alpha^T\mathbf{S}(\mathbf{P}_{\alpha,A}+\mathbf{P}_{\alpha,A}^T)\mathbf{SG}_\alpha\mathbf{T}_{\alpha,W}\boldsymbol{\alpha}_{\alpha,OO}^{-1}]^{YkXl}[\boldsymbol{\sigma}_{\alpha,YY}^{-1}\mathbf{C}_{\alpha,Y}^T\mathbf{G}_\alpha^T(\mathbf{S}-\mathbf{SP}_\alpha\mathbf{S})\mathbf{G}_\alpha\mathbf{C}_{\alpha,X}\boldsymbol{\sigma}_{\alpha,XX}^{-1}]^{Y\bar{t}X\bar{s}}\bigg]$$

For the case $\mathbf{G}_\alpha = \mathbf{M}_\alpha$ we have the following intermediate results that can be used to show that both (E.1) and (E.2) are zero:

$$[\sum_{ZW} \boldsymbol{\sigma}_{\alpha,OO}^{-1}\mathbf{T}_{\alpha,Z}^T\mathbf{G}_\alpha^T\mathbf{S}(\mathbf{P}_{\alpha,A}+\mathbf{P}_{\alpha,A}^T)\mathbf{SG}_\alpha\mathbf{T}_{\alpha,W}\boldsymbol{\alpha}_{\alpha,OO}^{-1}]^{XlYk} = (\boldsymbol{\sigma}_{\alpha,OO}^{-1})^{XlYk}[\delta_A^X + \delta_A^Y] \quad (E.3)$$

$$[\sum_Z \boldsymbol{\sigma}_{\alpha,OO}^{-1}\mathbf{T}_{\alpha,Z}^T\mathbf{G}_\alpha^T\mathbf{S}(\mathbf{P}_{\alpha,A}+\mathbf{P}_{\alpha,A}^T)\mathbf{S}(\mathbf{I}-\mathbf{P}_\alpha\mathbf{S})\mathbf{G}_\alpha\mathbf{C}_{\alpha,Y}\boldsymbol{\sigma}_{\alpha,YY}^{-1}]^{XlY\bar{t}} = [\boldsymbol{\sigma}_{\alpha,OO}^{-1}\boldsymbol{\sigma}_{\alpha,OY}\boldsymbol{\sigma}_{\alpha,YY}^{-1}]^{XlY\bar{t}}[\delta_A^Y - \delta_A^X]$$

$$(E.4)$$

$$[\boldsymbol{\sigma}_{\alpha,XX}^{-1}\mathbf{C}_{\alpha,X}^T\mathbf{G}_\alpha^T(\mathbf{I}-\mathbf{SP}_\alpha)\mathbf{S}(\mathbf{P}_{\alpha,A}+\mathbf{P}_{\alpha,A}^T)\mathbf{S}(\mathbf{I}-\mathbf{P}_\alpha\mathbf{S})\mathbf{G}_\alpha\mathbf{C}_{\alpha,Y}\boldsymbol{\sigma}_{\alpha,YY}^{-1}]^{X\bar{s}Y\bar{t}} \quad (E.5)$$

$$= [\delta_A^Y + \delta_A^X][\boldsymbol{\sigma}_{\alpha,XX}^{-1}(\boldsymbol{\sigma}_{\alpha,XY} - \boldsymbol{\sigma}_{\alpha,XO}\boldsymbol{\sigma}_{\alpha,OO}^{-1}\boldsymbol{\sigma}_{\alpha,OY})\boldsymbol{\sigma}_{\alpha,YY}^{-1}]^{X\bar{s}Y\bar{t}}$$

Appendix F: Linearly Dependent SCFMI Population Derivatives

The first and second derivatives of populations with respect to the degrees of freedom in the linearly dependent SCFMI subspaces, $\{X'\}$, described in the text can be obtained by replacing unprimed SCFMI subspace labels in (E.1) and (E.2) with their primed

23

counterparts ($\mathbf{C}_{\alpha,X'} \leftarrow \mathbf{C}_{\alpha,X}$ etc). The statements made in the text assume that the vectors spanning the primed subspaces are constructed in a specific way (II.32) from unprimed $\mathbf{G}_\alpha = \mathbf{M}_\alpha$ SCFMI sub-spaces. Rewriting the primed variants of (E.1) and (E.2) in terms of Mulliken-domain attributed vectors yields:

$$\frac{\partial \text{Pop}_{\alpha,A}}{\partial(\Delta_{\alpha,X'})_{X\hat{p}C\hat{q}}}\bigg|_{\Delta_\alpha=0} = \sum_E [\delta_{E\hat{r}}^{X\hat{p}}\delta_{X\hat{i}}^{C\hat{q}} - \delta_{X\hat{i}}^{X\hat{p}}\delta_{E\hat{r}}^{C\hat{q}}][\sum_{Z'}(\boldsymbol{\sigma}_{\alpha,OO})^{-1}\mathbf{T}_{\alpha,Z'}^T\mathbf{G}_\alpha^T\mathbf{S}(\mathbf{P}_{\alpha,A}+\mathbf{P}_{\alpha,A}^T)\mathbf{S}(\mathbf{I}-\mathbf{P}_\alpha\mathbf{S})\mathbf{G}_\alpha\mathbf{C}_{\alpha,X'}(\boldsymbol{\sigma}_{\alpha,X'X'})^{-1}]^{X\hat{i}E\hat{r}}$$

(F.1)

$$\frac{\partial^2 \text{Pop}_{\alpha,A}}{\partial(\Delta_{\alpha,X'})_{X\hat{p}C\hat{q}}\partial(\Delta_{\alpha,Y'})_{Y\hat{n}D\hat{o}}}\bigg| \quad \text{(F.2)}$$

$$+\delta_{Y'}^{X'}\frac{1}{2}\sum_{EFG}[+\delta_{E\hat{t}}^{X\hat{p}}\delta_{F\hat{u}}^{C\hat{q}}\delta_{G\hat{v}}^{Y\hat{n}}\delta_{X\hat{k}}^{D\hat{o}} - \delta_{E\hat{t}}^{X\hat{p}}\delta_{F\hat{u}}^{C\hat{q}}\delta_{G\hat{v}}^{D\hat{o}}\delta_{X\hat{k}}^{Y\hat{n}} - \delta_{E\hat{t}}^{C\hat{q}}\delta_{F\hat{u}}^{X\hat{p}}\delta_{G\hat{v}}^{Y\hat{n}}\delta_{X\hat{k}}^{D\hat{o}} + \delta_{E\hat{t}}^{C\hat{q}}\delta_{F\hat{u}}^{X\hat{p}}\delta_{G\hat{v}}^{D\hat{o}}\delta_{X\hat{k}}^{Y\hat{n}}$$

$$+\delta_{E\hat{t}}^{Y\hat{n}}\delta_{F\hat{u}}^{D\hat{o}}\delta_{G\hat{v}}^{X\hat{p}}\delta_{X\hat{k}}^{C\hat{q}} - \delta_{E\hat{t}}^{Y\hat{n}}\delta_{F\hat{u}}^{D\hat{o}}\delta_{G\hat{v}}^{C\hat{q}}\delta_{X\hat{k}}^{X\hat{p}} - \delta_{E\hat{t}}^{D\hat{o}}\delta_{F\hat{u}}^{Y\hat{n}}\delta_{G\hat{v}}^{X\hat{p}}\delta_{X\hat{k}}^{C\hat{q}} + \delta_{E\hat{t}}^{D\hat{o}}\delta_{F\hat{u}}^{Y\hat{n}}\delta_{G\hat{v}}^{C\hat{q}}\delta_{X\hat{k}}^{X\hat{p}}]$$

$$\times[\sum_{Z'}\boldsymbol{\sigma}_{\alpha,OO}^{-1}\mathbf{T}_{\alpha,Z'}^T\mathbf{G}_\alpha^T\mathbf{S}(\mathbf{P}_{\alpha,A}+\mathbf{P}_{\alpha,A}^T)\mathbf{S}(\mathbf{I}-\mathbf{P}_\alpha\mathbf{S})\mathbf{G}_\alpha\mathbf{C}_{\alpha,X'}\boldsymbol{\sigma}_{\alpha,X'X'}^{-1}]^{X\hat{k}E\hat{t}}(\boldsymbol{\sigma}_{\alpha,X'X'}^{-1})^{F\hat{u}G\hat{v}}$$

$$+\sum_{EF}[\delta_{X\hat{l}}^{X\hat{p}}\delta_{E\hat{s}}^{C\hat{q}}\delta_{Y\hat{k}}^{Y\hat{n}}\delta_{F\hat{t}}^{D\hat{o}} - \delta_{X\hat{l}}^{X\hat{p}}\delta_{E\hat{s}}^{C\hat{q}}\delta_{Y\hat{k}}^{D\hat{o}}\delta_{F\hat{t}}^{Y\hat{n}} - \delta_{X\hat{l}}^{C\hat{q}}\delta_{E\hat{s}}^{X\hat{p}}\delta_{Y\hat{k}}^{Y\hat{n}}\delta_{F\hat{t}}^{D\hat{o}} + \delta_{X\hat{l}}^{C\hat{q}}\delta_{E\hat{s}}^{X\hat{p}}\delta_{Y\hat{k}}^{D\hat{o}}\delta_{F\hat{t}}^{Y\hat{n}}]$$

$$\times\bigg[(\boldsymbol{\sigma}_{\alpha,OO}^{-1})^{X\hat{l}Y\hat{k}}[\boldsymbol{\sigma}_{\alpha,X'X'}^{-1}\mathbf{C}_{\alpha,X'}^T\mathbf{G}_\alpha^T(\mathbf{I}-\mathbf{S}\mathbf{P}_\alpha)\mathbf{S}(\mathbf{P}_{\alpha,A}+\mathbf{P}_{\alpha,A}^T)\mathbf{S}(\mathbf{I}-\mathbf{P}_\alpha\mathbf{S})\mathbf{G}_\alpha\mathbf{C}_{\alpha,Y'}\boldsymbol{\sigma}_{\alpha,Y'Y'}^{-1}]^{E\hat{s}F\hat{t}}$$

$$-[\sum_{Z'}\boldsymbol{\sigma}_{\alpha,OO}^{-1}\mathbf{T}_{\alpha,Z'}^T\mathbf{G}_\alpha^T\mathbf{S}(\mathbf{P}_{\alpha,A}+\mathbf{P}_{\alpha,A}^T)\mathbf{S}(\mathbf{I}-\mathbf{P}_\alpha\mathbf{S})\mathbf{G}_\alpha\mathbf{C}_{\alpha,Y'}\boldsymbol{\sigma}_{\alpha,Y'Y'}^{-1}]^{X\hat{l}F\hat{t}}[\sum_{W'}\boldsymbol{\sigma}_{\alpha,OO}^{-1}\mathbf{T}_{\alpha,W'}^T\boldsymbol{\Gamma}_\alpha\mathbf{C}_{\alpha,X'}\boldsymbol{\sigma}_{\alpha,X'X'}^{-1}]^{Y\hat{k}E\hat{s}}$$

$$-[\sum_{Z'}\boldsymbol{\sigma}_{\alpha,OO}^{-1}\mathbf{T}_{\alpha,Z'}^T\mathbf{G}_\alpha^T\mathbf{S}(\mathbf{P}_{\alpha,A}+\mathbf{P}_{\alpha,A}^T)\mathbf{S}(\mathbf{I}-\mathbf{P}_\alpha\mathbf{S})\mathbf{G}_\alpha\mathbf{C}_{\alpha,X'}\boldsymbol{\sigma}_{\alpha,X'X'}^{-1}]^{Y\hat{k}E\hat{s}}[\sum_{W'}\boldsymbol{\sigma}_{\alpha,OO}^{-1}\mathbf{T}_{\alpha,W'}^T\boldsymbol{\Gamma}_\alpha\mathbf{C}_{\alpha,Y'}\boldsymbol{\sigma}_{\alpha,Y'Y'}^{-1}]^{X\hat{l}F\hat{t}}$$

$$-[\sum_{Z'W'}\boldsymbol{\sigma}_{\alpha,OO}^{-1}\mathbf{T}_{\alpha,Z'}^T\mathbf{G}_\alpha^T\mathbf{S}(\mathbf{P}_{\alpha,A}+\mathbf{P}_{\alpha,A}^T)\mathbf{S}\mathbf{G}_\alpha\mathbf{T}_{\alpha,W'}\boldsymbol{\alpha}_{\alpha,OO}^{-1}]^{Y\hat{k}X\hat{l}}[\boldsymbol{\sigma}_{\alpha,Y'Y'}^{-1}\mathbf{C}_{\alpha,Y'}^T\mathbf{G}_\alpha^T(\mathbf{S}-\mathbf{S}\mathbf{P}_\alpha\mathbf{S})\mathbf{G}_\alpha\mathbf{C}_{\alpha,X'}\boldsymbol{\sigma}_{\alpha,X'X'}^{-1}]^{F\hat{t}E\hat{s}}\bigg]$$

In these expressions, matching primed and un-primed subspace indices, X' and X, are coupled because all occupied vectors in subspace X' have Mulliken-domain labels X. This coupling of indices is also described by (II.32). The gradient and Hessian for the degrees of freedom present in the un-primed subspace SCFMI are recovered for $X = C$ and $Y = D$ in the above, and these can be shown using the results for important cases below to both be zero. The derivatives for the newly introduced de-localization degrees of freedom are given by $X \neq C$ and $Y \neq D$. Orthogonal Mulliken domains refers to the case where the columns of $\mathbf{M}_\alpha$ are orthogonal, and thus at our initial condition we can choose without loss of generality to have $\boldsymbol{\sigma}_{\alpha,OO}$, $\boldsymbol{\sigma}_{\alpha,XX}$, $\boldsymbol{\sigma}_{\alpha,X'X'}$, and $\boldsymbol{\mu}_\alpha$ all $\mathbf{I}$.

$$[\sum_{Z'W'}\boldsymbol{\sigma}_{\alpha,OO}^{-1}\mathbf{T}_{\alpha,Z'}^T\mathbf{G}_\alpha^T\mathbf{S}(\mathbf{P}_{\alpha,A}+\mathbf{P}_{\alpha,A}^T)\mathbf{S}\mathbf{G}_\alpha\mathbf{T}_{\alpha,W'}\boldsymbol{\alpha}_{\alpha,OO}^{-1}]^{Y\hat{k}X\hat{l}} = (\boldsymbol{\sigma}_{\alpha,OO}^{-1})^{Y\hat{k}X\hat{l}}[\delta_A^X+\delta_A^Y] \qquad \text{(F.3)}$$

$$[\sum_{Z'}\boldsymbol{\sigma}_{\alpha,OO}^{-1}\mathbf{T}_{\alpha,Z'}^T\mathbf{G}_\alpha^T\mathbf{S}(\mathbf{P}_{\alpha,A}+\mathbf{P}_{\alpha,A}^T)\mathbf{S}(\mathbf{I}-\mathbf{P}_\alpha\mathbf{S})\mathbf{G}_\alpha\mathbf{C}_{\alpha,Y'}\boldsymbol{\sigma}_{\alpha,Y'Y'}^{-1}]^{X\hat{l}F\hat{t}} \quad \text{(F.4)}$$

$$= \left[\sum_Z\boldsymbol{\sigma}_{\alpha,OO}^{-1}\mathbf{T}_{\alpha,Z}^T\boldsymbol{\mu}_\alpha\right]_{\bullet A\tilde{\gamma}}^{X\hat{l}\,\bullet}\left((\mathbf{C}_{\alpha,A})_{\bullet Aq}^{A\tilde{\gamma}\bullet}(\boldsymbol{\sigma}_{\alpha,Y'Y'}^{-1})^{A\hat{q}F\hat{t}} - \sum_E[(\mathbf{I}-\delta_E^Y)\delta_A^Y\boldsymbol{\mu}_{\alpha,YY}^{-1}\boldsymbol{\mu}_{\alpha,YE}\mathbf{C}_{\alpha,E}]_{\bullet Eq}^{A\tilde{\gamma}\bullet}(\boldsymbol{\sigma}_{\alpha,Y'Y'}^{-1})^{E\hat{q}F\hat{t}}\right)$$

24

$$-\delta_A^X \left[\boldsymbol{\sigma}_{\alpha,OO}^{-1}\boldsymbol{\sigma}_{\alpha,OY'}\boldsymbol{\sigma}_{\alpha,Y'Y'}^{-1}\right]^{X\hat{I}F\hat{t}}$$

$$= (\text{CASE: } F = Y) \rightarrow [\boldsymbol{\sigma}_{\alpha,OO}^{-1}\boldsymbol{\sigma}_{\alpha,OA}]_{\bullet Aq}^{X\hat{I}\,\bullet}(\boldsymbol{\sigma}_{\alpha,Y'Y'}^{-1})^{A\hat{q}F\hat{t}} - \delta_A^X[\boldsymbol{\sigma}_{\alpha,OO}^{-1}\boldsymbol{\sigma}_{\alpha,OY'}\boldsymbol{\sigma}_{\alpha,Y'Y'}^{-1}]^{X\hat{I}F\hat{t}}$$

$$= (\text{CASE: } F = Y = X) \rightarrow 0$$

$$= (\text{CASE: Orthogonal Mulliken Domains}) \rightarrow 0$$

$$[\boldsymbol{\sigma}_{\alpha,X'X'}^{-1}\mathbf{C}_{\alpha,X'}^T\mathbf{G}_\alpha^T(\mathbf{I} - \mathbf{SP}_\alpha)\mathbf{S}(\mathbf{P}_{\alpha,A} + \mathbf{P}_{\alpha,A}^T)\mathbf{S}(\mathbf{I} - \mathbf{P}_\alpha\mathbf{S})\mathbf{G}_\alpha\mathbf{C}_{\alpha,Y'}\boldsymbol{\sigma}_{\alpha,Y'Y'}^{-1}]^{E\hat{s}F\hat{t}} = \quad (\text{F.5})$$

$$+ \sum_G (\boldsymbol{\sigma}_{\alpha,X'X'}^{-1})^{E\hat{s}G\hat{v}}[\mathbf{C}_{\alpha,G}^T(\mathbf{I} - \mathbf{S}\boldsymbol{\Phi}_{\alpha,X})\mathbf{S}(\mathbf{I} - \mathbf{PS})\mathbf{C}_{\alpha,A}]_{GvAu}(\boldsymbol{\sigma}_{\alpha,Y'Y'}^{-1})^{A\hat{u}F\hat{t}}$$

$$+ \sum_H (\boldsymbol{\sigma}_{\alpha,X'X'}^{-1})^{E\hat{s}A\hat{v}}[\mathbf{C}_{\alpha,A}^T(\mathbf{I} - \mathbf{SP})\mathbf{S}(\mathbf{I} - \boldsymbol{\Phi}_{\alpha,Y}\mathbf{S})\mathbf{C}_{\alpha,H}]_{AvHu}(\boldsymbol{\sigma}_{\alpha,Y'Y'}^{-1})^{H\hat{u}F\hat{t}}$$

$$+ \delta_E^X(\boldsymbol{\sigma}_{\alpha,X'X'}^{-1})^{E\hat{s}X\hat{v}}[\mathbf{C}_{\alpha,X}^T\mathbf{S}(\mathbf{I} - \mathbf{PS})\mathbf{C}_{\alpha,A}]_{XvAu}(\boldsymbol{\sigma}_{\alpha,Y'Y'}^{-1})^{A\hat{u}F\hat{t}}$$

$$+ \delta_F^Y(\boldsymbol{\sigma}_{\alpha,X'X'}^{-1})^{E\hat{s}A\hat{v}}[\mathbf{C}_{\alpha,A}^T(\mathbf{I} - \mathbf{SP})\mathbf{S}\mathbf{C}_{\alpha,Y}]_{AvYu}(\boldsymbol{\sigma}_{\alpha,Y'Y'}^{-1})^{Y\hat{u}F\hat{t}}$$

$$+ \sum_G \delta_F^Y\delta_A^Y(\boldsymbol{\sigma}_{\alpha,X'X'}^{-1})^{E\hat{s}G\hat{v}}[\mathbf{C}_{\alpha,G}^T(\mathbf{I} - \mathbf{S}\boldsymbol{\Phi}_{\alpha,X})\mathbf{S}(\mathbf{I} - \mathbf{PS})\mathbf{C}_{\alpha,Y}]_{GvYu}(\boldsymbol{\sigma}_{\alpha,Y'Y'}^{-1})^{Y\hat{u}F\hat{t}}$$

$$+ \sum_H \delta_E^X\delta_A^X(\boldsymbol{\sigma}_{\alpha,X'X'}^{-1})^{E\hat{s}X\hat{v}}[\mathbf{C}_{\alpha,X}^T(\mathbf{I} - \mathbf{SP})\mathbf{S}(\mathbf{I} - \boldsymbol{\Phi}_{\alpha,Y}\mathbf{S})\mathbf{C}_{\alpha,H}]_{XvHu}(\boldsymbol{\sigma}_{\alpha,Y'Y'}^{-1})^{H\hat{u}F\hat{t}}$$

$$- \sum_H \delta_E^X\delta_A^Y(\boldsymbol{\sigma}_{\alpha,X'X'}^{-1})^{E\hat{s}X\hat{v}}[\mathbf{C}_{\alpha,X}^T\mathbf{S}(\mathbf{I} - \mathbf{PS})\boldsymbol{\Phi}_{\alpha,Y}\mathbf{S}\mathbf{C}_{\alpha,H}]_{XvHu}(\boldsymbol{\sigma}_{\alpha,Y'Y'}^{-1})^{H\hat{u}F\hat{t}}$$

$$- \sum_G \delta_F^Y\delta_A^X(\boldsymbol{\sigma}_{\alpha,X'X'}^{-1})^{E\hat{s}G\hat{v}}[\mathbf{C}_{\alpha,G}^T\mathbf{S}\boldsymbol{\Phi}_{\alpha,X}(\mathbf{I} - \mathbf{SP})\mathbf{S}\mathbf{C}_{\alpha,Y}]_{GvYu}(\boldsymbol{\sigma}_{\alpha,Y'Y'}^{-1})^{Y\hat{u}F\hat{t}}$$

$$- \sum_{GH} (\boldsymbol{\sigma}_{\alpha,X'X'}^{-1})^{E\hat{s}G\hat{v}}[\mathbf{C}_{\alpha,G}^T\mathbf{S}(\delta_A^X\boldsymbol{\Phi}_{\alpha,X}(\mathbf{I} - \mathbf{SP}) + \delta_A^Y(\mathbf{I} - \mathbf{PS})\boldsymbol{\Phi}_{\alpha,Y})\mathbf{S}\mathbf{C}_{\alpha,H}]_{GvHu}(\boldsymbol{\sigma}_{\alpha,Y'Y'}^{-1})^{H\hat{u}F\hat{t}}$$

$$+ \delta_F^Y\delta_E^X(\delta_A^X + \delta_A^Y)(\boldsymbol{\sigma}_{\alpha,X'X'}^{-1})^{E\hat{s}X\hat{v}}[\mathbf{C}_{\alpha,X}^T(\mathbf{I} - \mathbf{SP})\mathbf{S}\mathbf{C}_{\alpha,Y}]_{XvYu}(\boldsymbol{\sigma}_{\alpha,Y'Y'}^{-1})^{Y\hat{u}F\hat{t}}$$

$$+ \sum_{GH} (\delta_A^X + \delta_A^Y)(\boldsymbol{\sigma}_{\alpha,X'X'}^{-1})^{E\hat{s}G\hat{v}}[\mathbf{C}_{\alpha,G}^T\mathbf{S}\boldsymbol{\Phi}_{\alpha,X}(\mathbf{I} - \mathbf{SP})\mathbf{S}\boldsymbol{\Phi}_{\alpha,Y}\mathbf{S}\mathbf{C}_{\alpha,H}]_{GvHu}(\boldsymbol{\sigma}_{\alpha,Y'Y'}^{-1})^{H\hat{u}F\hat{t}}$$

$$= (\text{CASE: } E = X, F = Y) \rightarrow$$

$$+ \delta_A^Y(\boldsymbol{\sigma}_{\alpha,X'X'}^{-1})^{E\hat{s}X\hat{v}}[\mathbf{C}_{\alpha,X}^T\mathbf{S}(\mathbf{I} - \mathbf{PS})\mathbf{C}_{\alpha,A}]_{XvAu}(\boldsymbol{\sigma}_{\alpha,Y'Y'}^{-1})^{A\hat{u}F\hat{t}}$$

$$+ \delta_A^X(\boldsymbol{\sigma}_{\alpha,X'X'}^{-1})^{E\hat{s}A\hat{v}}[\mathbf{C}_{\alpha,A}^T(\mathbf{I} - \mathbf{SP})\mathbf{S}\mathbf{C}_{\alpha,Y}]_{AvYu}(\boldsymbol{\sigma}_{\alpha,Y'Y'}^{-1})^{Y\hat{u}F\hat{t}}$$

$$= (\text{CASE: Orthogonal Mulliken Domains}) \rightarrow 2\delta_{A\hat{a}}^{E\hat{s}}\delta_{A\hat{a}}^{F\hat{t}}$$

[1] M.J.S. Phipps, T. Fox, C.S. Tautermann, and C.-K. Skylaris, Chem. Soc. Rev., Advance Article, DOI: 10.1039/c4cs00375f (2015).

[2] R.Z. Khaliullin, E.A. Cobar, R.C. Lochan, A.T. Bell, and M. Head-Gordon, J. Phys. Chem. A, **111**,8753 (2007).

[3] Q. Wu, P.W. Ayers, and Y. Zhang, J. Chem. Phys., **131**,164112 (2009).

[4] Q. Wu, J. Chem. Phys., **140**,244109 (2014).

[5] S. Rybak, B. Jeziorski, and K. Szalewicz, J. Chem. Phys., **95**,6576 (1991).

[6] B. Jeziorski, R. Moszynski, and K. Szalewicz, Chem. Rev., **94**,1887 (1994).

[7] A. Misquitta, B. Jeziorski, and K. Szalewicz, Phys. Rev. Lett., **91**,033201 (2003).

[8] A.J. Misquitta, R. Podeszwa, B. Jeziorski, and K. Szalewicz, J. Chem. Phys., **123**,214103 (2005).

[9] P.S. Zuchowski, R. Podeszwa, R. Moszyski, B. Jeziorski, and K. Szalewicz, J. Chem. Phys., **129**,084101 (2008).

[10] M. von Hopffgarten and G. Frenking, WIREs Comput. Mol. Sci., **0**,1 (2011).

[11] F.M. Bickelhaupt and E.J. Baerends, in *Reviews in Computational Chemistry* (John Wiley & Sons, Inc., Hoboken, NJ, USA, 2000), Vol. 15, pp. 1-86.

[12] A. Krapp, F.M. Bickelhaupt, and G. Frenking, Chem. Eur. J., **12**,9196 (2006).

[13] T. Ziegler and A. Rauk, Theor. Chem. Acc., **46**,1 (1977).

[14] T. Ziegler and A. Rauk, Inorg. Chem., **18**,1558 (1979).

[15] M.P. Mitoraj, A. Michalak, and T. Ziegler, J. Chem. Theory Comput., **5**,962 (2009).

[16] S. Ndambuki and T. Ziegler, Int. J. Quantum Chem., **113**,753 (2013).

[17] P. Reinhardt, J. Piquemal, and A. Savin, J. Chem. Theory Comput., **4**,2020 (2008).

[18] P. Su and H. Li, J. Chem. Phys., **131**,014102 (2009).

[19] P. Su, H. Liu, and W. Wu, J. Chem. Phys., **137**,034111 (2012).

[20] P. Su, Z. Jiang, Z. Chen, and W. Wu, J. Phys. Chem. A, **118**,2531 (2014).

[21] M. Mandado and J.M. Hermida-Ramón, J. Chem. Theory Comput., **7**,633 (2011).

[22] I.C. Hayes and A.J. Stone, Mol. Phys., **53**,83 (1984).

[23] A.J. Stone and A.J. Misquitta, Chem. Phys. Lett., **473**,201 (2009).

[24] A.J. Misquitta, J. Chem. Theory Comput., **9**,5313 (2013).

[25] A.E. Reed and F. Weinhold, J. Chem. Phys., **78**,4066 (1983).

[26] A.E. Reed, L.A. Curtiss, and F. Weinhold, Chem. Rev., **88**,899 (1988).

[27] E.D. Glendening and A. Streitwieser, J. Chem. Phys., **100**,2900 (1994).

[28] G.K. Schenter and E.D. Glendening, J. Phys. Chem., **100**,17152 (1996).

[29] E.D. Glendening, J. Phys. Chem. A, **109**,11936 (2005).

[30] K. Kitaura and K. Morokuma, Int. J. Quantum Chem., **x**,325, (1976).

[31] K. Morokuma, Acc. Chem. Res., **10**,294 (1977).

[32] W. Chen and M.S. Gordon, J. Phys. Chem., **100**,14316 (1996).

[33] D.G. Fedorov and K. Kitaura, J. Comput. Chem., **28**,222 (2007).

[34] M.C. Green, D.G. Fedorov, K. Kitaura, J.S. Francisco, and L.V. Slipchenko, J. Chem. Phys., **138**,074111 (2013).

[35] J. Korchowiec and T. Uchimaru, J. Phys. Chem. A, **102**,6682 (1998).

[36] J. Korchowiec and T. Uchimaru, J. Chem. Phys., **112**,1623 (2000).

[37] K. Kitaura, T. Sawai, T. Asada, T. Nakano, and M. Uebayasi Chem. Phys. Lett., **312**,319 (1999).

[38] K. Kitaura, E. Ikeo, T. Asada, T. Nakano, and M. Uebayasi, Chem. Phys. Lett, **313**,701 (1999).

[39] M.S. Gordon, J.M. Mullin, S.R. Pruitt, J.B. Roskop, L.V. Slipchenko, and J.A. Boatz, J. Phys. Chem. B, **113**,9646 (2009).

[40] M.S. Gordon, D.G. Fedorov, and S.R. Pruitt, and L.V. Slipchenko, Chem. Rev., **112**,632 (2012).

[41] Y. Mochizuki, K. Fukuzawa, A. Kato, S. Tanaka, K. Kitaura, and T. Nakano, Chem. Phys. Lett., **410**,247 (2005).

[42] P.S. Bagus, K. Hermann, and C.W. Jr. Bauschlicher, J. Chem. Phys., **80**,4378 (1984).

[43] W.J. Stevens and W.H. Fink,

[44] **139**,15 (1987).

[45] J. Řezáč and A. de la Lande, J. Chem. Theory Comput., **11**,528 (2015).

[46] H. Stoll, G. Wagenblast, and H. Preuß, Theor. Chem. Acc., **57**,169 (1980).

[47] E. Gianinetti, M. Raimondi, and E. Tornaghi, Int. J. Quantum Chem., **60**,157 (1996).

[48] Y. Mo, J. Gao, and S.D. Peyerimhoff, J. Chem. Phys., **122**,5530 (2000).

[49] Y. Mo, L. Song, and Y. Lin, J. Phys. Chem. A, **111**,8291 (2007).

[50] Y. Mo, P. Bao, and J. Gao, Phys. Chem. Chem. Phys., **13**,6760 (2011).

[51] S.N. Steinmann, C. Corminboeuf, W. Wu, and Y. Mo, J. Phys. Chem. A, **115**,5467 (2011).

[52] R.Z. Khaliullin, M. Head-Gordon, and A.T. Bell, J. Chem. Phys., **124**,204105 (2006).

[53] R.Z. Khaliullin, A.T. Bell, and M. Head-Gordon, J. Chem. Phys., **128**,184112 (2008).

[54] P.R. Horn, E.J. Sundstrom, T.A. Baker, and M. Head-Gordon, J. Chem. Phys., **138**,134119 (2013).

[55] P. De Silva and J. Korchowiec, J. Comput. Chem., **32**,1054 (2011).

[56] K. Yamada and N. Koga, Theor. Chem. Acc., **131**,1178 (2012).

[57] T. Nagata, O. Takahashi, K. Saito, and S. Iwata, J. Chem. Phys., **115**,3553 (2001).

[58] A.J. Stone, Chem. Phys. Lett., **211**,101 (1993).

[59] T.K. Ghanty, V.N. Staroverov, P.R. Koren, and E.R. Davidson, J. Am. Chem. Soc., **122**,1210 (2000).

[60] R.J. Azar, P.R. Horn, E.J. Sundstrom, and M. Head-Gordon, J. Chem. Phys., **138**,084102 (2013).

[61] M. Head-Gordon, P.E. Maslen, and C.A. White, J. Chem. Phys., **108**,616 (1998).

[62] A. Stone, *The Theory of Intermolecular Forces. 2nd ed.* (Oxford University Press, Oxford, 2013), pp. 285.

[63] P. Pulay, J. Comput. Chem., **3**,556 (1982).

[64] J. Nocedal and S.J. Wright, *Numerical Optimization* (Springer-Verlag, New York, 1999), pp. 224-227.

[65] T. Van Voorhis and M. Head-Gordon, Mol. Phys., **100**,1713 (2002).

[66] F. Weinhold and J.E. Carpenter, J. Mol. Struct.: THEOCHEM, **165**,189 (1988).

[67] B.C. Carlson and J.M. Keller, Phys. Rev., **105**,102 (1957).

[68] W. Liang and M. Head-Gordon, J. Phys. Chem. A, **108**,3206 (2004).

[69] W. Liang and M. Head-Gordon, J. Chem. Phys., **120**,10379 (2004).

[70] Y. Shao, L.F. Molnar, Y. Jung, J. Kussmann, C. Ochsenfeld, S.T. Brown, A.T.B. Gilbert, L.V. Slipchenko, S.V. Levchenko, D.P O'Neill, R.A. DiStasio, R.C. Lochan, T. Wang, G.J.O. Beran, N.A. Besley, J.M. Herbert, C.Y. Lin, T. Van Voorhis, S.H. Chien, A. Sodt, R.P. Steele, V.A. Rassolov, P.E. Maslen, P.P. Korambath, R.D. Adamson, B. Austin, J. Baker, E.F.C. Byrd, H. Dachsel, R.J. Doerksen, A. Dreuw, B.D. Dunietz, A.D. Dutoi, T.R. Furlani, S.R. Gwaltney, A. Heyden, S. Hirata, C. Hsu, G. Kedziora, R.Z. Khalliulin, P. Klunzinger, A.M. Lee, M.S. Lee, W. Liang, I. Lotan, N. Nair, B. Peters, E.I. Proynov, P.A. Pieniazek, Y.M. Rhee, J. Ritchie, E. Rosta, C.D. Sherrill, A.C. Simmonett, J.E. Subotnik, H.L. Woodcock, W. Zhang, A.T. Bell, A.K. Chakraborty, D.M. Chipman, F.J. Keil, A. Warshel, W.J. Hehre, H.F. Schaefer, J. Kong, A.I. Krylov, P.M.W. Gill, and M. Head-Gordon, Phys. Chem. Chem. Phys., **8**,3172 (2006).

[71] Y. Shao, Z. Gan, E. Epifanovsky, A.T.B. Gilbert, M. Wormit, J. Kussmann, A.W. Lange, A. Behn, J. Deng, X. Feng, D. Ghosh, M. Goldey, P.R. Horn, L.D. Jacobson, I. Kaliman, R.Z. Khaliullin, T. Kuś, A. Landau, J. Liu, E.I. Proynov, Y.M. Rhee, R.M. Richard, M.A. Rohrdanz, R.P. Steele, E.J. Sundstrom, H.L. Woodcock, P.M. Zimmerman, D. Zuev, B. Albrecht, E. Alguire, B. Austin, G.J.O. Beran, Y.A. Bernard, E. Berquist, K. Brandhorst, K.B. Bravaya, S.T. Brown, D. Casanova, C. Chang, Y. Chen, S.H. Chien, K.D. Closser, D.L. Crittenden, M. Diedenhofen, R.A. DiStasio, H. Do, A.D. Dutoi, R.G. Edgar, S. Fatehi,

26

L. Fusti-Molnar, A. Ghysels, A. Golubeva-Zadorozhnaya, J. Gomes, M.W.D. Hanson-Heine, P.H.P. Harbach, A.W. Hauser, E.G. Hohenstein, Z.C. Holden, T. Jagau, H. Ji, B. Kaduk, K. Khistyaev, J. Kim, J. Kim, R.A. King, P. Klunzinger, D. Kosenkov, T. Kowalczyk, C.M. Krauter, K.U. Lao, A. Laurent, K.V. Lawler, S.V. Levchenko, C.Y. Lin, F. Liu, E. Livshits, R.C. Lochan, A. Luenser, P. Manohar, S.F. Manzer, S. Mao, N. Mardirossian, A.V. Marenich, S.A. Maurer, N.J. Mayhall, E. Neuscamman, C.M. Oana, R. Olivares-Amaya, D.P. ONeill, J.A. Parkhill, T.M. Perrine, R. Peverati, A. Prociuk, D.R. Rehn, E. Rosta, N.J. Russ, S.M. Sharada, S. Sharma, D.W. Small, A. Sodt, T. Stein, D. Stück, Y. Su, A.J.W. Thom, T. Tsuchimochi, V. Vanovschi, L. Vogt, O. Vydrov, T. Wang, M.A. Watson, J. Wenzel, A. White, C.F. Williams, J. Yang, S. Yeganeh, S.R. Yost, Z. You, I.Y. Zhang, X. Zhang, Y. Zhao, B.R. Brooks, G.K.L. Chan, D.M. Chipman, C.J. Cramer, W.A. Goddard, M.S. Gordon, W.J. Hehre, A. Klamt, H.F. Schaefer, M.W. Schmidt, C.D. Sherrill, D.G. Truhlar, A. Warshel, X. Xu, A. Aspuru-Guzik, R. Baer, A.T. Bell, N.A. Besley, J. Chai, A. Dreuw, B.D. Dunietz, T.R. Furlani, S.R. Gwaltney, C. Hsu, Y. Jung, J. Kong, D.S. Lambrecht, W. Liang, C. Ochsenfeld, V.A. Rassolov, L.V. Slipchenko, J.E. Subotnik, T. Van Voorhis, J.M. Herbert, A.I. Krylov, P.M.W. Gill, and M. Head-Gordon, Mol. Phys., **113**,184 (2015).

[72] T.H. Jr. Dunning, J. Chem. Phys., **90**,1007 (1989).

[73] R.A. Kendall, T.H. Jr. Dunning, and R.J. Harrison, J. Chem. Phys., **96**,6796 (1992).

[74] A.D. Becke, J. Chem. Phys., **98**,5648 (1993).

[75] C. Lee, W. Yang, and R.G. Parr, Phys. Rev. B, **37**,785 (1988).

[76] A.D. Becke, Phys. Rev. A, **38**,3098 (1988).

[77] S. Grimme, J. Comput. Chem., **27**,1787 (2006).

[78] S. Grimme, J. Antony, S. Ehrlich, and H. Krieg, J. Chem. Phys., **132**,154104 (2010).

[79] A. Fornili, M. Sironi, and M. Raimondi, J. Mol. Struct.: THEOCHEM, **632**,157 (2003).

[80] M. Sironi, A. Genoni, M. Civera, S. Pieraccini, and M. Ghitti, Theor. Chem. Acc., **117**,685 (2007).

27